

# Bio-inspired Protein-Based and Activatable Adhesion Systems

Christina Heinritz, Xuen J. Ng, and Thomas Scheibel\*

Adhesives are in general chemically or physically sticky substances used to join surfaces. In case of gluing biological and living substrates, there is a need for bioadhesives that meet requirements such as biocompatibility, non-toxicity, and degradability. Inspiration for bioadhesives is found in nature, where distinct mussels, sandcastle worms, barnacles, caddisfly larvae, spiders, and glowworms amongst others, use mainly protein-based glues for various purposes. There is a great selection of reviews and books covering the use of various bioadhesives in various applications, but here the focus lies on advances in the development of bio-inspired protein-based adhesives for biomedical applications.

intrusive and invasive procedure. During the last century, adhesives have also been employed for medical purposes. However, to date, both for internal and external wounds, sutures still describe the gold standard for surgical procedures. Although there have been efforts to develop degradable and anti-microbial sutures,<sup>[3]</sup> the use of sutures, in general, is time-consuming and requires high precision and well-trained personnel.<sup>[4]</sup> In this regard, staples and clips offer a quicker solution to closing wounds. In either case, however, the physical penetration of healthy tissue creates a possible gate for pathogens to enter the body, thus increasing

## 1. Introduction

Adhesives have been used by humans for thousands of years, attested by wall carvings in Theben dating 3300 years back depicting the gluing of veneer, which are sheets of wood.<sup>[1]</sup> From making tools to the use for constructions and buildings in the form of cement, adhesives are a versatile and maybe even indispensable tool to bond surfaces of a variety of materials, geometries, and topographies, which is otherwise not possible by other joining methods.<sup>[2]</sup> The use of adhesives is also associated with a less

the risk of infection. Pathogen intrusion then might require additional intervention after wound healing, in case the materials used are non-absorbable.<sup>[5]</sup> In this context, and with the emergence of the first commercial cyanoacrylate-based synthetic tissue adhesive known as Eastman 910 in the late 1960s, the application of adhesives for wound treatment has gained increasing interest.

Cyanoacrylates (CA) are a class of synthetic adhesives that undergo rapid polymerization in contact with weak bases such as water or blood, which can cause trouble in case of the treatment of internal wounds, as the rapid hardening will form a layer with weak adhesive surface properties, limiting its application to external wound treatment, but not inside the body.<sup>[6]</sup> The biocompatibility of CAs is low but can be improved by increasing the length of ester side chains,<sup>[7]</sup> yielding derivatives such as *n*-butyl-cyanoacrylates (Histoacryl and Glubran2) and 2-octyl-cyanoacrylates (Dermabond), which are nowadays mostly used for wound sealing. Still, there are valid concerns concerning toxic degradation products such as cyanoacetate and formaldehyde, causing inflammatory responses.<sup>[8]</sup> Evading the toxicity issue, polyethylene-glycol (PEG)-based adhesives have increasingly been used, such as the commercially available ProGel, CoSeal, DuraSeal, or FocalSeal. The highly modifiable chemistry of PEG-based systems allows tuning of the adhesive and cohesive properties, and those materials are further biocompatible and mostly biodegradable but display a strong swelling behavior, which can compromise their mechanical properties due to a decrease in crosslinking density or result in delamination of the gel made thereof caused by stress of the hydrogel interface.<sup>[9]</sup>

Biocompatibility and biodegradability issues have shifted the course for exploring and developing new tissue adhesives toward natural and semi-synthetic systems. The global market size for tissue sealants and adhesives was valued at roughly \$2.7 billion in

C. Heinritz, X. J. Ng, T. Scheibel  
Chair of Biomaterials  
Engineering Faculty  
University of Bayreuth  
Prof.-Rüdiger-Bormann-Straße 1, 95447 Bayreuth, Germany  
E-mail: thomas.scheibel@bm.uni-bayreuth.de

T. Scheibel  
Bayreuth Center for Colloids and Interfaces (BZKG)  
Bavarian Polymer Institute (BPI)  
Bayreuth Center for Molecular Biosciences (BZMB)  
Bayreuth Center for Material Science (BayMAT)  
University of Bayreuth  
Universitätsstraße 30, 95447 Bayreuth, Germany  
T. Scheibel  
Faculty of Medicine  
University of Würzburg  
Pleicherwall 2, 97070 Würzburg, Germany

 The ORCID identification number(s) for the author(s) of this article can be found under <https://doi.org/10.1002/adfm.202303609>

© 2023 The Authors. Advanced Functional Materials published by Wiley-VCH GmbH. This is an open access article under the terms of the Creative Commons Attribution-NonCommercial License, which permits use, distribution and reproduction in any medium, provided the original work is properly cited and is not used for commercial purposes.

DOI: 10.1002/adfm.202303609

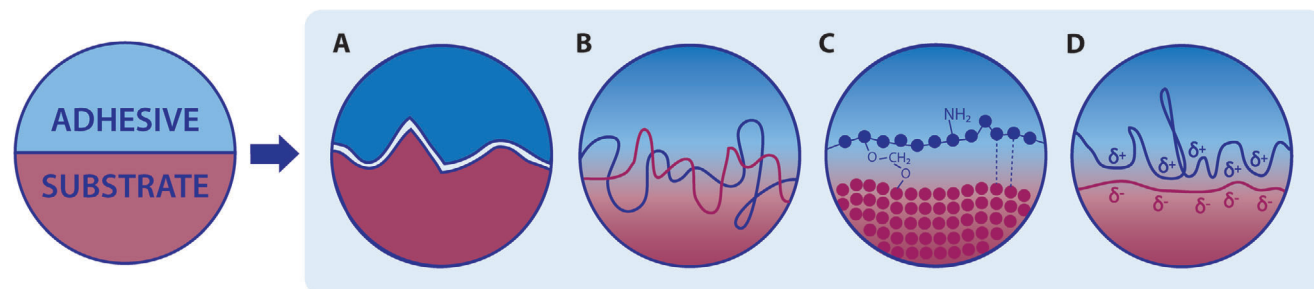


**Figure 1.** Mechanisms of bioadhesion. A) mechanical interlocking; B) chain entanglement; C) intermolecular bonding; and D) electrostatic bonding. Reproduced (Adapted) with permission.<sup>[12]</sup> Copyright 2018, Wiley-VCH GmbH.

2020 and is estimated to reach  $\approx$ \$5.2 billion by 2030 with a compound annual growth rate of 6.7%. Natural biological sealants and adhesives make a larger share in this section compared to synthetic and semi-synthetic systems, with this trend expected to continue in the future, considering the ongoing development of surgical sealants and adhesives.<sup>[10]</sup> Due to the increasing attention to these new materials, the term bioadhesive has been introduced. A bioadhesive is defined as a material used for joining two surfaces by interfacial forces, where one or both constitute living tissue, over an extended period of time.<sup>[11]</sup>

For the successful development of new adhesives, a comprehensive understanding of the underlying mechanisms is indispensable. In general, there are four mechanisms by which adhesion can occur (Figure 1).<sup>[12]</sup> There is A) non-specific physical adhesion such as mechanical interlocking, by which the adhesive infiltrates microscopic pores and cavities of the substrate, and the surface roughness or rather surface area is determining the adhesive strength. B) Chain entanglement is based on polymer chain mobility and respective physical entanglement, often seen among two polymer interfaces such as those of self-healing hydrogels, hence requiring amorphous polymer networks with low crystallinity. Then there is specific adhesion mediated by C) intermolecular chemical bonds between molecules of the adhesive and the surface. The forces arising from covalent, ionic, or metal-ion coordinated bonds are the strongest, while hydrogen bonds, dipole-dipole interactions, and Van der Waals forces provide less energy, however, can also play a significant role in case of high enough quantities. Lastly, there are D) electrostatic interactions mediated by oppositely charged surfaces. While all these interactions at the substrate-adhesive interface provide the basis of adhesion, an effective joint between two surfaces requires furthermore an adequate level of cohesion, denoting the internal strength of the adhesive material. The network can be held together by covalent bonding or non-covalent strategies, such as mechanical reinforcement by particles or fibrillar structures, self-assembly, or phase transitions, and should be able to withstand movement and shear stress.<sup>[13]</sup> The performance of an adhesive is determined substantially by a balanced combination of adhesive and cohesive forces.

There is general consent that the ideal bioadhesive has to reliably hold tissue in place and aid in healing and regeneration of the tissue. Hence, it has to be biocompatible, non-immunogenic, and should undergo enzymatic or hydrolytic degradation within several weeks, at which point it should have been infiltrated and gradually replaced by body-own tissue or cells. If the material

does not degrade, it could create a barrier between tissue interfaces and prevent the tissue to interconnect. As adhesives are also aimed to replace suturing processes, they further require ease of application to reduce surgery time and should be applicable in physiological conditions, including wet surfaces, which is particularly challenging. Interfacial water prevents the contact of functional groups of adhesive and substrate, hence significantly reducing the adhesive strength if not even completely preventing it. The removal or displacement of interfacial water is a key element of bioadhesion and the main to-be-solved issue for most common glues, as their performance is significantly decreased in a wet environment.<sup>[14]</sup>

Nature can teach us how the demanding (bio)adhesion requirements could be met. Natural glues are used by many animals and plants for various purposes like attachment, locomotion, home construction, mating, defense, and prey hunting (Figure 2).<sup>[15]</sup> Differences are observed regarding the adhesive mechanism, as some organisms use permanent adhesion, like mussels and barnacles that secrete a hardening cement, whereas other adhesive strategies are non-permanent, for instance, used by starfish or geckos for attachment and locomotion.<sup>[16]</sup> Moreover, physical adhesion can take place in a dry environment, which, according to many studies, is caused by very fine hairy structures in the nano- or micrometer-scale, maximizing the surface area of contact and, thus, is derived from Van der Waals interactions.<sup>[17]</sup> In wet environments, other adhesion mechanisms are necessary, and many adhesives, although showing a strong adhesion on dry surfaces, fail underwater, because the interfacial hydration layer needs to be absorbed or repelled prior to emergence of adhesive interactions.<sup>[18]</sup>

Mimicking the multifaceted natural adhesion mechanisms enables the exploration of bio-inspired adhesives, displaying an attractive alternative to synthetic glues with respect to mechanical and medical requirements. For a broad overview of bio-based and bio-inspired adhesives from animals and plants, we would like to recommend the recent review from Lutz et al.<sup>[15]</sup> Moreover, Rathi et al. provide a good overview of protein adhesives and glues, which are commercially available or in clinical trials, most of which are based on either fibrin, collagen, or albumin from human or bovine sources.<sup>[12]</sup> The focus of this review is on protein-based adhesives inspired by various animals. First, possible natural adhesive mechanisms will be elucidated as basis for the current state of research on bio-inspired adhesives. Then, triggered adhesion-on-demand will be highlighted to provide insights into specifically activatable bioadhesives.

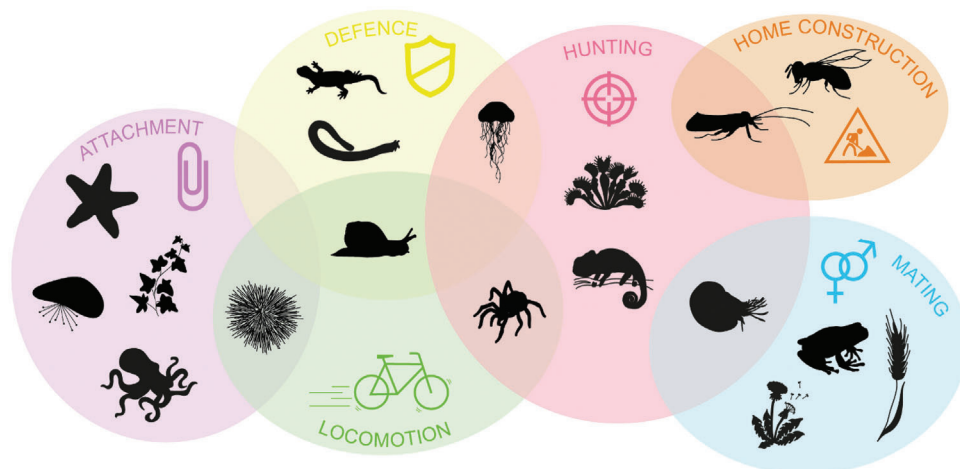


**Figure 2.** Schematic representation of applications of sticky substances produced by animals and plants for attachment (purple), defense (yellow), locomotion (green), hunting (pink), home construction (orange), and mating (blue). Reproduced under the terms of the Attribution-NonCommercial-NoDerivatives 4.0 International (CC BY-NC-ND 4.0) license.<sup>[15]</sup> Copyright 2022, the Authors, published by Elsevier.

## 2. Protein-Based Natural Adhesives

Natural protein-based adhesives are used for different purposes. For example, the permanent underwater adhesion of adult mussels and barnacles is mediated by a proteinaceous secrete.<sup>[19]</sup> Sandcastle worms build their protective retreat using protein-based cement.<sup>[20]</sup> Spiders and glowworms rely on sticky silk threads for capture of food,<sup>[21]</sup> whereas caddisfly larvae have adapted their adhesive silk to their habitat in the freshwater environment.<sup>[22]</sup> These and more adhesive strategies can be found under water and ashore, underlining the complexity and diversity of bioadhesion. Li et al. summarized the protein-mediated bioadhesion, especially in marine organisms, considering some shared generic characteristics:<sup>[23]</sup> 1) Protein biosynthesis, packaging, and release of adhesives are clearly localized in secretory cells. 2) Proteins display a distinctive amino acid composition, which might be closely related to their adhesive function. 3) Functional domains – functional structural units in a protein sequence – are often conserved. 4) Proteins contain abundant post-translational modifications (like hydroxylation, phosphorylation, and glycosylation) and oxidative crosslinking. 5) Often enzymes are involved for efficient adhesion.

Importantly, adhesives of most organisms show different adhesive mechanisms (**Figure 3**), including rather complex combinations thereof to produce the most suitable bioadhesive adapted to the particular needs.

### 2.1. DOPA-Based Adhesion Used by Marine Mussels

The most prominent and extensively studied model system for protein-based bioadhesion in nature and a frequently used model system derives from mussels, which are able to anchor to diverse surfaces even under wet ambient conditions. Several mussels form so-called byssus filaments (threads), which prevent dislodgement by wave-induced water motion as well as hungry predators and adhere the mussel effectively to almost any underwater surface. Among different mussel species, the number, size, and mechanical properties of byssal threads can vary, influencing

the strength of the anchorage.<sup>[24]</sup> Each thread is produced individually by the foot of the mussel within 30 s to 8 min, one at a time, and connects with an adhesive plaque at the distal end to the substrate surface.<sup>[19a]</sup> Further, mussel byssus provides a mechanical gradient to connect the soft mussel tissue with hard surfaces (e.g. rocks), with increasing stiffness toward the substrate in order to avoid deformational damage of the softer tissue.<sup>[25]</sup> This particular property has also inspired the design of new materials and is discussed elsewhere.<sup>[26]</sup>

The formation of a byssus thread starts with the mussel foot pressing against the target surface and temporarily sticking itself using suction force by lifting the ceiling of the pad, thus creating a cavity with negative pressure.<sup>[19a]</sup> Shielded from the surrounding seawater, the pH, ionic strength, and redox conditions are adjusted prior to deposition of the thread components within a ventral groove.<sup>[27]</sup> Three major glands, the phenol (plaque formation), collagen (thread core formation), and accessory gland (cuticle formation) are subsequently involved in production of the byssus filament.<sup>[28]</sup> The filament is composed of collagen-like proteins (preCols) embedded in several matrix proteins including the so-called mussel foot protein (Mfp), of which new variants are still occasionally identified.<sup>[28]</sup> Six of the Mfps are found in the adhesive plaque.<sup>[29]</sup> Common to all is the abundance of post-translational modifications, which occur to variable degrees depending on the species and protein, like hydroxylation of tyrosine ( $\tau$ -3,4-dihydroxyphenylalanine, DOPA; highest content in Mfp-5 with  $\approx 30$  mol%), sometimes paired with phosphorylated serine (pSer) or 4-hydroxylated arginine (**Table 1**).<sup>[30]</sup> As DOPA contributes particularly to bioadhesion,<sup>[31]</sup> its mechanism will be discussed in more detail below.

DOPA is a catechol-derivate and comprises a benzene ring with two neighboring hydroxy groups.<sup>[32]</sup> Its molecular interactions are diverse and range from electrostatic interactions, hydrogen bonds, hydrophobic interactions,  $\pi$ - $\pi$  stacking, cation- $\pi$  interactions, and metal coordination to covalent bonds (**Figure 4**).<sup>[33]</sup> The catechol-metal complexation is of high strength, close to a covalent bond, and enhances adhesion on metal-containing surfaces. It is also connected to high cohesion, since metal ions

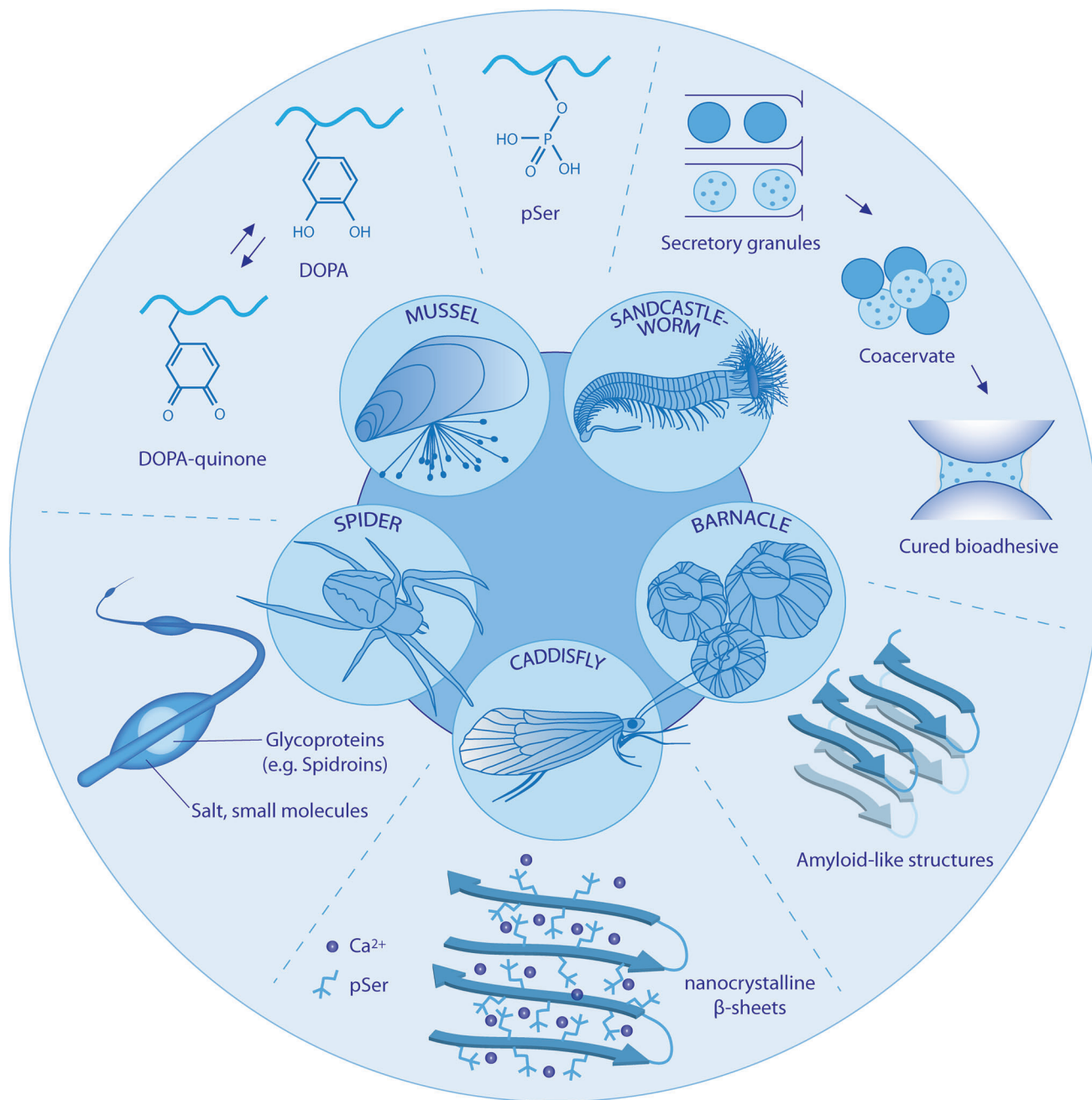


**Figure 3.** Schematic overview of described animals and their main adhesion mechanism. Mussels predominantly use adhesive interactions based on post-translational modifications like L-3,4-dihydroxyphenylalanine (DOPA) or phosphorylated serine (pSer). Those are also found in sandcastle worms, whose polyelectrolytic adhesive proteins form coacervates to successfully apply the glue to the target area. The proteinaceous cement of barnacles comprises amyloid-like structures. Fibrillar protein assembly is also observed in the silk of several animals, for instance, the silk of caddisfly larvae. Rich in pSer, the phosphorylated sites interact with Calcium ions to form  $\beta$ -sheet crystalline regions. Ecribellate spiders modify their silk web with adhesive droplets from their aggregate gland, consisting of specific glycoproteins, including spidroins.

like  $\text{Ca}^{2+}$  and  $\text{Fe}^{3+}$  are present in the mussel byssus and, depending on the concentration, contribute to crosslinking due to the interaction of multiple DOPA residues with one metal ion.<sup>[34]</sup> Metal complexation is a reversible interaction, leading to good self-healing ability and high extensibility of the byssus cuticle. While metal coordination is favored at neutral to basic pH, the

catechol group has a high affinity to form bidentate hydrogen bonds to oxide and amine groups on a surface, which is presumably the dominating adhesion force at acidic pH on surfaces like mica, minerals, metal oxides, and oxygen-containing polymers. Hydrogen atoms are donated to acceptors such as oxygen, nitrogen, and fluorine, or in summation to hydrophilic



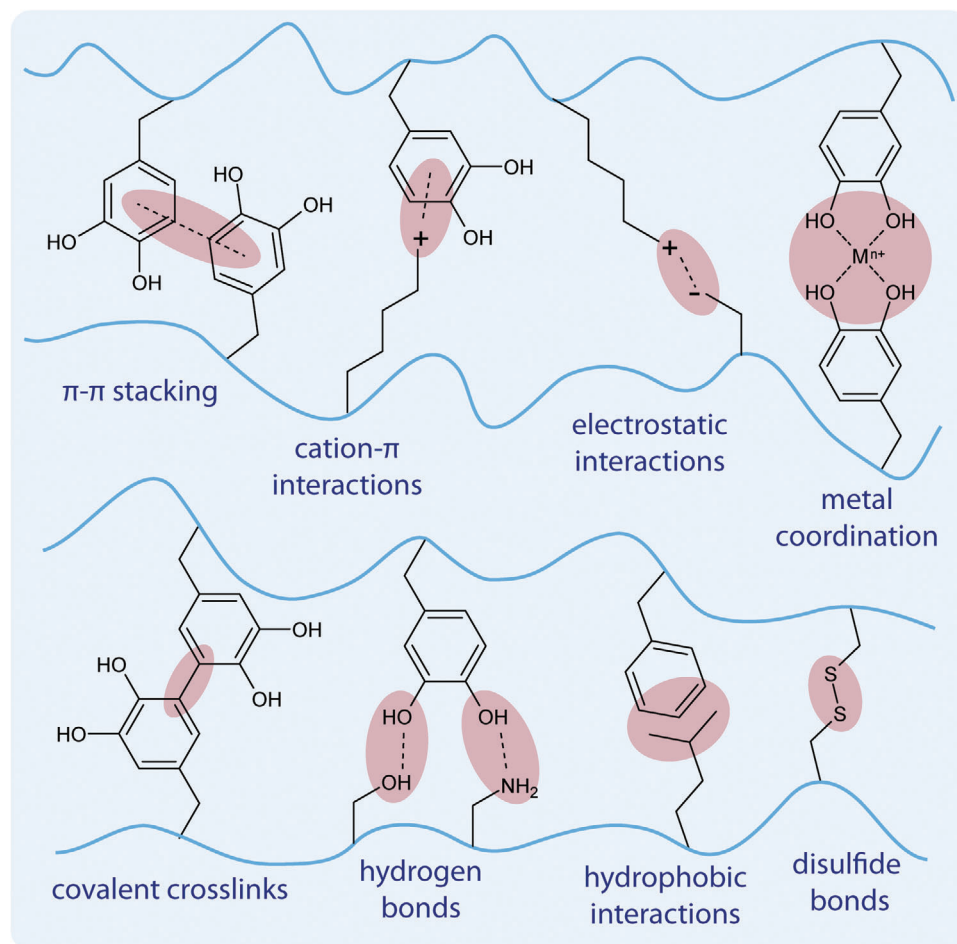


**Figure 4.** Overview of the proposed different adhesive and cohesive molecular interactions found in proteins from e.g. mussels and sandcastle worms. Reproduced (Adapted) under the terms of the Attribution-NonCommercial (CC-BY-NC) license.<sup>[39]</sup> Copyright 2018, John Wiley and Sons.

residues.<sup>[33]</sup> Furthermore, the aromatic moiety can form  $\pi$ - $\pi$  interactions: organic surfaces with other electron-rich  $\pi$ -systems evoke stacking of the aromatic rings, e.g. graphite or graphene.<sup>[32]</sup> Even stronger than these  $\pi$ - $\pi$  interactions are cation- $\pi$  interactions between the aromatic system and cations (e.g.  $\text{Li}^+$ ,  $\text{Na}^+$ ,  $\text{K}^+$ ,  $\text{NH}_4^+$ ). Analysis of the amino acid content of Mfps also revealed an increased occurrence of lysine residues, which led to the hypothesis of a synergistic effect of lysine and DOPA in close proximity.<sup>[36]</sup> Importantly, in addition to lysine, other charged amino acid residues and phosphorylation may support adhesion through electrostatic interactions with charged surface groups.<sup>[19a]</sup>

A hallmark characteristic of DOPA-chemistry is its dependence on redox conditions. The loss of one electron leads to DOPA-semiquinone, and further loss of a second one to DOPA-quinone, resulting in reduced surface adhesion.<sup>[31,37]</sup> According to Cooper, seawater with high oxygen content has a positive redox potential and, therefore, a high affinity to accept electrons.<sup>[19a,38]</sup> Moreover, spontaneous auto-oxidation of DOPA is promoted by alkaline conditions around pH 8, but can also be initiated by chemical oxidants like periodate and catechol oxidase enzymes.

The mussel overcomes these unfavorable effects by the aforementioned shielding from the environment during the plaque formation process and the initial adjustment of the conditions. In addition, the cysteine-rich Mfp-6 is secreted at the interface, which converts DOPA-quinone back to DOPA via oxidation of its thiol groups and, at the same time, partially forms disulfide bridges through oxidation, which cross-links the protein glue.<sup>[37,39]</sup> Mfp-6 can partially rescue DOPA, but cannot completely prevent the formation of DOPA-quinone. However, this is not necessary, because oxidized DOPA can form covalent bonds with a second DOPA molecule and, thus, acts as a cross-linker contributing to cohesion. The mussel thereby masters the balance between cohesion and adhesion, as too high levels of oxidation of DOPA lead to failure of surface adhesion, while too little oxidation-mediated cross-linking leads to failure of cohesive forces.<sup>[40]</sup> At the same time, control of the oxidation level enables controlled adhesion and detachment of the mussel.

The abundance of different interaction mechanisms of DOPA makes it a highly versatile system, allowing mussels to interact with almost any type of surface, both hydrophobic and

hydrophilic, and at both acidic and basic pH.<sup>[41]</sup> The mussel foot proteins and their DOPA-based adhesion mechanism, hence, have inspired the design of a multitude of biomimetic adhesives.

## 2.2. Coacervation in Sandcastle Worms

Another prominent example of wet adhesion derives from *P. californica*, commonly known as sandcastle worm. The worm, as well as other relatives of the species of polychaetes, uses a proteinaceous glue to assemble mineral particles and build tubular shells, which in their entity form almost reef-like structures in the coastal region and provide the worms with protection from predators as well as environmental stress caused by waves and desiccation.<sup>[42]</sup> Mineral particles like sand grains and calcareous shell fragments floating in the marine water are captured and transported by the animal with tentacles inwards to the so-called building organ, where a protein-based adhesive fluid is secreted to join the bits, also termed cement.<sup>[43]</sup> Molecular analysis of the proteins revealed that the sandcastle worm, like the mussel, exploits the post-translational modified DOPA.<sup>[44]</sup> More prominent than the overall 2–3 mol% DOPA, the whole glue shows a high content of phosphorylated serine (pSer, ≈30 mol%), with individual proteins even comprising >80% serine in their primary sequence (Table 1).<sup>[42b,44–45]</sup> pSer is a second post-translational modification widely found in marine adhesive proteins and occurs moreover in sequences, which have similarities to mineral-binding motifs in proteins of the bone extracellular matrix,<sup>[46]</sup> suggesting an adaptation to adhesion on calcareous surfaces.<sup>[30a,47]</sup> The consequence of the high phosphorylation level, which occurs predominantly in Pc3 proteins, is the anionic net charge. On the other hand, a closer look at the residual proteins Pc1, Pc2, Pc4, and Pc5 reveals a polycationic character, due to the enrichment in arginine, lysine, and histidine.<sup>[48]</sup> Overall, ≈50% of amino acids are charged at physiological pH, and the separation of charges into macromolecules led to the theory that complex coacervation – liquid-liquid phase separation of components of opposite charges – plays a role in the adhesion process of sandcastle worms,<sup>[49]</sup> which is highlighted in more detail below.

The gland tissue producing the glue components and storing them in granular secretory vesicles is composed of two major cell types: one type is producing homogeneous granules, the other heterogeneous granules, a designation that is due to the different morphologies and staining behavior.<sup>[50]</sup> The result is a local separation of the glue components into two adhesive modules, which constitutes an important feature of the adhesive system of sandcastle worms in addition to the high polyelectrolyte content.<sup>[49]</sup> The oppositely charged macromolecules are stored as pairs: The cationic proteins Pc2 and 5 are combined with negatively charged sulfated polysaccharides in the homogeneous granules, while the heterogeneous granules comprise the polyphosphate proteins Pc3B and polyampholytic proteins Pc3A along with the polycationic proteins Pc1 and 4.<sup>[49]</sup> Additional high concentrations of Mg<sup>2+</sup> ions in the heterogeneous granules are thought to neutralize the negative charge of the phosphate groups.<sup>[49]</sup> In each of the granules, the electrostatic association of oppositely charged polyelectrolytes causes partial expulsion of water and small bound counter ions driven by the associated gain in entropy (Figure 5). This leads to a concentration of the polymers into a densely

packed phase-separated fluid – a phenomenon known as complex coacervation – that consists of a polymer-enriched liquid phase (the coacervate phase), and a polymer-depleted dilute phase (the remaining solution).<sup>[20,49–51]</sup> If, as in case of the sandcastle worm, two or more individual polyelectrolytes of opposite charge interact with each other, the process is called complex coacervation. However, liquid-liquid phase separation may also occur with only one, amphiphathic polymer, which is then referred to as simple coacervation. The components of the sandcastle worm cement stay in the complex coacervated state, and components of homogeneous and heterogeneous granules are strictly separated until secretion from the gland. After release, the granules rupture, probably caused by mechanical stress, leading the contents to fuse with little mixing and harden into a porous solid foam.<sup>[49]</sup> The transition from the coacervated fluid phase into a solid is promoted by small changes in the solution conditions, like ionic strength and the pH jumping from acidic in the packaging system to basic in the seawater.<sup>[43]</sup> At a seawater pH of 8.2, histidine residues (pK<sub>a</sub> ≈6.5) would become deprotonated and, thus, result in a loss of positive charge, setting free their counter phosphate groups. The phosphate groups in turn enter into new interactions with the remaining positively charged Ca<sup>2+</sup> and Mg<sup>2+</sup> ions, with the interactions being more similar to ionic bonds, resulting in spontaneous hardening of the glue.<sup>[43]</sup> Additionally, a catechol oxidase enzyme is also found in both homogeneous and heterogeneous granules and catalyzes the oxidation of the DOPA-side chains into DOPA-quinone, which are subsequently cross-linked covalently during curing of the glue.<sup>[20]</sup> In summary, the coacervate processing provides an intermediate for the storage and delivery of aqueous underwater bioadhesives without dispersion, which is also used by mussels.<sup>[52]</sup> The state is accompanied by excellent wet coating and adhesive properties, caused by the low interfacial tension of the coacervate and good surface wetting ability in water.<sup>[53]</sup>

## 2.3. Phosphorylated Serine in the Glue of Caddisfly Larvae

Caddisflies (order *Trichoptera*) spend most of their lifecycle in the larval stage. Caddisfly larvae live in freshwater habitats where they feed, mature, and pupate underwater.<sup>[30b]</sup> All suborders use adhesive silk for the construction of protective tube-like shelters, like the sandcastle worm, and for food procurement.<sup>[22]</sup> Related to moths like the domesticated silkworm, homologues of the silk have been identified.<sup>[54]</sup> In particular, the silk fiber is made of a nanofibrous core comprising two major fibroins: the heavy chain fibroin (H-fibroin) and light chain fibroin (L-fibroin), which are most likely connected by disulfide bridges.<sup>[55]</sup> H-fibroin makes up the largest proportion and consists of nonrepetitive N- and C-termini flanking a long, conserved core region. Other than silk from silkworms or spiders, caddisfly silk is not abundant in alanine but enriched in serine, which is extensively phosphorylated (13 mol% pSer in H-fibroin).<sup>[56]</sup> Since phosphoserines are commonly found in the adhesive secreted from marine organisms like mussels, sandcastle worms, and sea cucumbers, this obviously represents an adaptation to the aquatic environment.<sup>[57]</sup> Repeats of (pSX)<sub>n</sub>E motifs (pS = phosphorylated serine, X = hydrophobic or basic residue, n = 4 or 5, E = glutamic acid) and glycine-rich motifs conferring elasticity are located in the

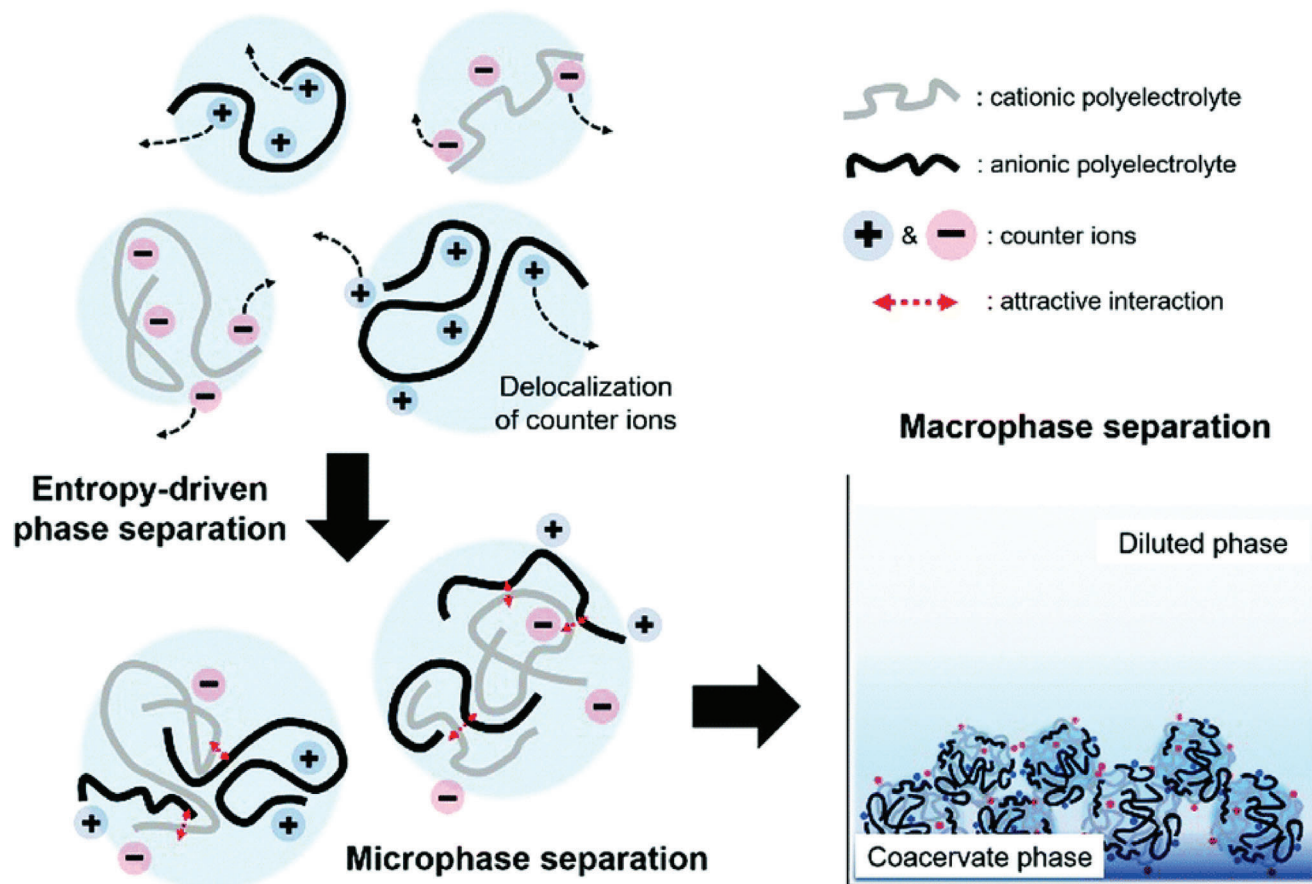


**Figure 5.** Schematic diagram of complex coacervation resulting from a two-step process, namely the charge neutralization of polyelectrolytes by attractive interactions (such as electrostatic, van der Waals, hydrophobic interactions, and hydrogen bonding) and the gain in entropy by the delocalization and release of bound counter ions. The result is macrophase separation yielding a concentrated polymer phase (the coacervate) and the equilibrium solution (the diluted phase). Reproduced with permission.<sup>[51a]</sup> Copyright 2005, Royal Society of Chemistry.

central core region (Table 1).<sup>[22,58]</sup> Multiple studies support the proposed nanofibril core structure of  $\text{Ca}^{2+}$ -bridged phosphoserines, forming a rigid  $\beta$ -sheet-like crystalline region.<sup>[22,56,59]</sup> Antiparallel  $\beta$ -hairpins are thought to be electrostatically stabilized by calcium ions, resulting in mechanical stiffness and tensile strength of the silk fibers.<sup>[60]</sup> Furthermore, the silk fibers are coated with a layer of glycoproteins and peroxidase.<sup>[56]</sup> Initial surface adhesion is mediated by the fuzzy glycoprotein layer via intermolecular interactions such as chain entanglement, electrostatic interactions, or hydrogen bonds, but then the peroxidase can catalyze di-tyrosine crosslinking to covalently connect tyrosine residues from the peripheral fiber layer with phenolic groups from surface absorbed organic compounds and, thus, support both cohesion and adhesion.<sup>[61]</sup>

#### 2.4. Amyloid-Like Proteins in Barnacle Adhesives

Barnacles as sessile adults exhibit a strong permanent attachment and form a protective calcified shell. They adhere strongly to any suitable underwater surface, which constitutes a severe problem in shipping. Barnacle settlement, also termed barnacle fouling, significantly increases frictional resistance of ships and,

thus, drives up fuel consumption, resulting in economic loss.<sup>[62]</sup> For their adhesion, barnacles use a type of cement with  $\approx 90\%$  protein content,<sup>[63]</sup> and not all of the proteins have yet been fully characterized. No evidence has been found so far for the above-mentioned post-translational modifications (neither DOPA<sup>[63b,64]</sup> nor pSer<sup>[65]</sup>), but the proteins comprise lots of polar amino acids and a varying amount of cysteine (Cys) depending on the species. In addition to its primary protein composition, the barnacle adhesion mechanism differs from other marine organisms like the previously discussed mussel and sandcastle worm in its secretion process. A single cell type in the cement gland is responsible for the production and packaging of glue components in secretory granules.<sup>[66]</sup> Secretion is a slow process, and solidification of the cement, which has been discussed to include enzymatic crosslinking,<sup>[67]</sup> takes several hours reducing the risk of premature curing.<sup>[68]</sup> Since the current understanding of barnacle adhesion still includes controversial aspects such as the absence of intermolecular covalent crosslinking,<sup>[19b,67]</sup> the question arises as to the origin of the adhesive and cohesive force.

One component possibly involved could be highly insoluble amyloid-like protein fibrils,<sup>[63b]</sup> which were detected through specific staining methods for their characteristic cross- $\beta$  structures (using the dyes Congo red and Thioflavin T). Moreover, atomic

force microscopy imaging and spectroscopic methods confirmed nanofibrils and major  $\beta$ -sheet content.<sup>[69]</sup> Amyloid fibrils are highly ordered, typically unbranched, and structurally consist of  $\beta$ -strands aligned perpendicular to the fiber axis, which self-assemble from soluble proteins.<sup>[70]</sup> This particular type of protein assembly is associated in the human body with pathogenic conditions like Alzheimer's or Parkinson's disease.<sup>[71]</sup> As a bio-based material, amyloid fibrils are characterized, among others, to possess high mechanical strength and stability against degradation.<sup>[69a]</sup> This specific structural fold is also effectively used by other organisms for adhesion (e.g. prokaryotic curli fibers).<sup>[72]</sup>

Best studied is the cement of the acorn barnacle *M. rosa*, which consists of five different proteins.<sup>[19b]</sup> One of the examined proteins, CP-20, which is thought to interact at the substrate interface alongside a second protein, is enriched in charged amino acids (42 mol%) as well as Cys (17 mol%) (Table 1). Using a recombinantly produced CP-20, So et al. proposed a dynamic interaction between the protein and calcite. They observed a disorder-to-order transition of CP-20 upon contact with crystalline calcite, which could initiate fibril self-assembly.<sup>[73]</sup> Structural protein characterization also revealed that 12 out of 32 Cys residues form intramolecular disulfide bonds to stabilize molecular folding. The remaining thiol groups are free to engage in other intermolecular interactions as a functional group and might assist in the barnacle adhesive mechanism on various surfaces.

## 2.5. Aggregate Silk from Orb-Weaving Spiders and Glowworms as Adhesives

The web of orb-weaving spiders is essentially a trap for small insects used for catching prey.<sup>[74]</sup> Orb-weavers (*Araneoidea*) rely on the strength of their major ampullate silk fibers used for the webs' frame and radii, and the spiral architecture of the flagelliform silk (forming the capture spiral) to absorb the kinetic energy from incoming insects, or, in other words, slow down or stop the insect in mid-flight.<sup>[74]</sup> From a mechanical point of view, the major ampullate silk fibers represent a unique combination of high tensile strength and elasticity, caused by the primary protein structure of its spidroins (MaSp1 and MaSp2). The proteins' core domains consist of highly repetitive motifs, of which poly-alanine regions are forming crystalline antiparallel  $\beta$ -sheets and are responsible for the high toughness, whereas less ordered glycine-rich sections contribute to the elasticity.<sup>[75]</sup> To hinder the prey from escaping the web, spiders originally produced dry cribellar capture threads, which were fixed in between major ampullate silks on top of thick core fibers, featuring thousands of fine fibrils on the surface and, thus, achieving adhesion more by physical entanglement paired with Van der Waals and hygroscopic interactions.<sup>[76]</sup> While this type of adhesion is still used by members of *Deinopoidea*, the modern orb-weaving spiders (>95% of orb weavers) have transitioned over 135 million years ago to use a liquid viscous glue placed onto the above-mentioned flagelliform silk, featuring chemical adhesion, hence yielding a greater stickiness relative to volume and increased extensibility at lower costs for the spider.<sup>[77]</sup> This co-called viscid silk is a composite material of highly hydrated flagelliform silk and adhesive droplets, leading to a combination of adhesiveness, extensibility, elastic-

ity, and strength. The flagelliform fibers are coated during spinning with the aqueous glue solution secreted by framing aggregate glands, thus also called aggregate glue.<sup>[78]</sup> The aqueous adhesive is secreted as a continuous coating of the fiber, absorbs water, and breaks spontaneously into regularly spaced droplets. When in contact with caught prey, the glue shows also viscoelastic solid properties, meaning that the droplets elongate in order to maintain a physical connection to the substrate.<sup>[79]</sup>

Chemical analysis revealed that the glue droplets consist of an anchoring granule, surrounded by a glycoprotein-containing inner layer and a more aqueous outer layer, which comprises low molecular weight compounds and salts.<sup>[80]</sup> The salts in the secreted droplets are hygroscopic and absorb water from the atmosphere and, thereby, support solvation of the glycoproteins via a salting-in effect.<sup>[80c,81]</sup> Consequently, spider silk glues are humidity responsive: high humidity increases adhesive strength, which is probably an adaptation related to the humid natural habitat of spiders.<sup>[82]</sup> The inner layer consists of two extensively O-glycosylated protein subunits, aggregate spider glue proteins (ASG) 1 and 2. Evidence was found that ASG2 belongs to the spidroin family with its characteristic repetitive amino acid sequence region (Table 1) flanked by conserved non-repetitive terminal domains and contributes to cohesion of the glue. Due to this finding the protein was re-named aggregate spidroin 1 (AgSp1).<sup>[21a,b]</sup> AGS1 displays an adhesive function, as the protein includes regions similar to chitin-binding domains, revealing optimal prerequisites for insect attachment,<sup>[21a,81]</sup> but there are still many unanswered questions regarding the exact adhesion mechanism.

The bioluminescent larvae of certain fungus gnats, commonly referred to as glowworms, have developed a similar strategy to catch prey.<sup>[21c]</sup> In their natural habitats, preferably dark and humid places like caves, glowworms construct a tubular nest of silk and an adhesive mucus. Attracted by their luminous abdomen, small insects are caught using long elastic silk threads hanging down from the nest. The glowworm silk reveals a crystalline cross- $\beta$ -sheet structure akin to amyloids and different from the antiparallel  $\beta$ -sheets in spider silk.<sup>[83]</sup> The adhesive mucus, in contrast to spiders where the flagelliform fibers are continuously coated, is placed in droplets selectively every 1–1.5 mm onto the fiber during fiber spinning. The glue droplets consist of  $\approx$ 1% of hygroscopic macromolecules and 99% volatile substances and, therefore, are more sensitive to humidity, as relative humidity of <80% leads to drying of the droplet and crystallization of the components.<sup>[84]</sup> However, the mechanism behind the adhesive property of the glowworm secretes still needs to be investigated.

## 3. Bio-Inspired Protein-Based Adhesive Systems

Given the variety of available natural mechanisms for effective dry and wet adhesion, a straightforward approach for the preparation of a bioadhesive would be the direct extraction of components from biological sources. Mussel foot proteins are a characteristic example, which has been extensively studied to date and exhibit strong adhesion ideally adapted to the aqueous environment. However, direct retrieval of Mfps by isolation and purification is very laborious with a low yield estimated at 1 g protein per 10 000 mussels, despite advanced processes.<sup>[92]</sup> Therefore, commercially available mussel adhesive protein (MAP)-based

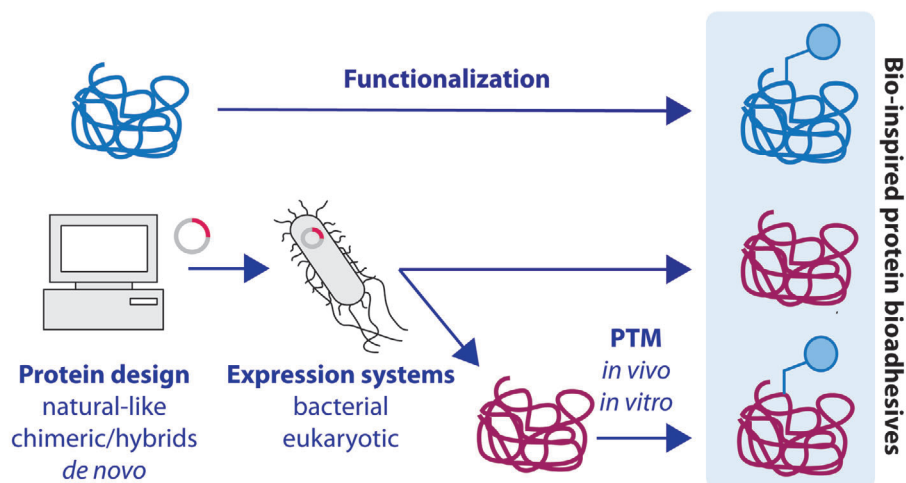


**Figure 6.** Overview of the described aspects of bio-inspired protein-based adhesives. Extracted natural proteins can be chemically or enzymatically functionalized (top). Bio-inspired adhesive proteins can be designed akin to the natural sequence, chimeric/hybrid, or de novo. The proteins are then produced in recombinant expression systems to either yield an already functional protein adhesive, or an intermediate, that can further undergo post-translation modifications (PTM) to obtain those functions (bottom).

adhesives comprise both extracted natural and recombinantly produced Mfps.<sup>[93]</sup>

Next to bioadhesives derived from natural sources, bio-inspired adhesives have clearly been on the rise in recent years. The design of new materials using natural adhesive motifs and structures enables control and fine-tuning of material properties as desired. The vast amount of literature discussing MAP and the development of mussel-inspired proteins reflects the main focus on DOPA and catechol groups, as it has been suggested to be the key factor for strong and rapid underwater adhesion not only in mussels. Research reports range from polydopamine materials (e.g. coatings)<sup>[94]</sup> and DOPA-containing short polypeptides to DOPA-functionalized polymers<sup>[95]</sup> and whole recombinant Mfps. A selection of these and other protein-based adhesive systems is discussed in the following section, divided into functionalized natural proteins and bioengineered recombinant protein adhesives (**Figure 6**). The adhesive strengths are typically not determined using standardized procedures. Thus, a direct comparison of the values should be treated with caution due to varying test set-ups with variable parameters, like amount and concentration of applied adhesive, used substrate, contact area, curing time and environment, and testing strain rate (**Table 2**).

### 3.1. Modified Proteins for Adhesives

Regenerated silk fibroin from *B. mori* is an FDA-approved protein, which is a well-suited biomaterial due to its biocompatibility, biodegradability, and mechanical properties. Silk fibroin, like other silk proteins, forms  $\beta$ -sheet-rich fibrils and comprises several amino acids with hydroxyl and acidic groups providing potential reaction sides for chemical modifications or crosslinking.<sup>[100]</sup> Therefore, it has been used to some extent for the development of several adhesive systems. Next to semi-synthetic approaches like the methacrylation of silk fibroin<sup>[115]</sup>

enabling photo-induced crosslinking, all-protein-based hydrogels have been developed by Zhao et al. using enzymatic crosslinking of intrinsic tyrosine residues.<sup>[100]</sup> Horse radish peroxidase introduced covalent bonds and, thus, promoted the formation of hydrogels, while the addition of  $\text{CaCl}_2$  led to electrostatic and chelation interactions of the silk fibroin with  $\text{Ca}^{2+}$  ions. The resulting hydrogel was reported to be conductive, self-adhesive, and stretchable leading to possible applications as wearable electronic sensors.

As reflected in the previous description of the natural adhesive systems, the implementation of the non-canonical amino acid DOPA into proteins is an attractive way to significantly increase surface adhesion. Chemical modification of proteins can be achieved using cross-linking between N-hydroxysuccinimide (NHS) and 1-ethyl-(3-dimethylaminopropyl) carbodiimide salt (EDC), reported in multiple works.<sup>[101–103]</sup> In this manner, DOPA-functionalized silk fibroin was produced by Liu et al. and blended with PEG to promote gelation into a hydrogel.<sup>[101]</sup> Adhesion studies on porcine skin revealed a high tensile strength in dry and wet conditions, which increased within 42 h due to cross-linking of oxidized DOPA-quinone during curing up to 0.5 MPa, and in vitro degradability of the glue was demonstrated using a protease. Another group improved the adhesive properties of its chemically DOPA-modified silk fibroin and accelerated the gelation process through the addition of genipin and  $\text{Fe}^{3+}$ .<sup>[102]</sup> The chelation of metal ions by catechol hydroxyl groups forming coordination bonds increased the adhesion using  $\text{Fe}^{3+}$  (248 kPa on porcine skin) more than using  $\text{Cu}^{2+}$ , which is explained by the ability of  $\text{Fe}^{3+}$  to coordinate with more hydroxyl groups. The other compound, genipin, acts as a cost-effective cross-linking agent. Both additives had a negligible negative impact on in vitro cell viability and had no effect at all on cell migration, thus indicating good biocompatibility as well as degradability of such adhesives, two important aspects for future biomedical applications.

**Table 2.** Overview of reported adhesive systems with a focus on adhesive properties.

Adhesive system	Method	Test conditions	Substrate	Curing conditions	adhesion strength/ adhesion energy	Ref.
<b>Reference materials</b>						
Cyanacrylate	Lap-shear test	ASTM F2255 (modified), 10 × 10 mm <sup>2</sup>	porcine skin	20 min, humid	≈0.075 MPa	[96]
	Lap-shear test	10 mm min <sup>-1</sup> or 40 mm min <sup>-1</sup> , 5 × 5 mm <sup>2</sup>	steel	12 h, dry	10.4 ± 0.6 MPa	[97]
Fibrin	End-to-end joint tensile test	10 mm min <sup>-1</sup> , 35 mm <sup>2</sup>	porcine skin	24 h, dry	2.01 ± 0.58 MPa	[98]
	End-to-end joint tensile test	10 mm min <sup>-1</sup> , 35 mm <sup>2</sup>	porcine skin	24 h, humid	0.96 ± 0.24 MPa	[96]
	Lap-shear test	ASTM F2255 (modified), 1 × 1 cm <sup>2</sup>	porcine skin	20 min – 24 h, humid	≈0.02 MPa	[98]
	End-to-end joint tensile test	10 mm min <sup>-1</sup> , 35 mm <sup>2</sup>	porcine skin	24 h, dry	0.54 ± 0.39 MPa	[98]
natural adhesives	End-to-end joint tensile test	10 mm min <sup>-1</sup> , 35 mm <sup>2</sup>	porcine skin	24 h, humid	0.43 ± 0.19 MPa	[98]
Mussel extracts ( <i>M. edulis</i> )	End-to-end joint tensile test	10 mm min <sup>-1</sup> , 35 mm <sup>2</sup>	porcine skin	24 h, dry	0.33 ± 0.17 MPa	[98]
Sandcastle worm cement ( <i>P. californica</i> )	End-to-end joint tensile test	10 mm min <sup>-1</sup> , 35 mm <sup>2</sup>	porcine skin	24 h, humid	0.93 ± 0.32 MPa	[99]
Modified natural proteins	Estimation based on “pull out” set-up	-	-	-	≈0.35 MPa	[99]
Silk fibroin + CaCl <sub>2</sub> + horse radish peroxidase	T-peel test	50 mm min <sup>-1</sup> , 10 × 20 mm <sup>2</sup>	porcine skin	12 h, 50% relative humidity (RH)	200 N m <sup>-1</sup>	[100]
DOPA-functionalized silk fibroin + PEG	Lap-shear test	ASTM F2255, 10 × 10 mm <sup>2</sup>	porcine skin	30 h, dry	0.448 ± 0.017 MPa	[101]
DOPA-functionalized silk fibroin + genipin + Fe <sup>3+</sup>	Lap-shear test	ASTM F2255, 10 × 10 mm <sup>2</sup>	porcine skin	42 h, wet	0.503 ± 0.017 MPa	[102]
	Lap-shear test	ASTM F2255, 1 mm min <sup>-1</sup> , 10 × 10 cm <sup>2</sup>	porcine skin	12 h, dry, 37 °C	0.248 ± 0.029 MPa	[103]
DOPA-functionalized pectin + β-lactoglobulin coacervate	Lap-shear test	50 mm min <sup>-1</sup> , 8 × 8 mm <sup>2</sup>	porcine skin	12 h, dry	≈1.48 MPa	[103]
	Lap-shear test	50 mm min <sup>-1</sup> , 8 × 8 mm <sup>2</sup>	glass	12 h, dry	≈0.4 MPa	[103]
	Lap-shear test	50 mm min <sup>-1</sup> , 8 × 8 mm <sup>2</sup>	porcine skin	12 h, wet	≈0.78 MPa	[103]
	Tensile test	5 mm min <sup>-1</sup> , 8 × 8 mm <sup>2</sup>	porcine skin	12 h, dry	≈0.72 MPa	[103]
	Tensile test	5 mm min <sup>-1</sup> , 8 × 8 mm <sup>2</sup>	glass	12 h, dry	≈0.54 MPa	[103]
Silk fibroin + tannic acid	T-peel test	5 mm min <sup>-1</sup>	porcine skin	12 h, dry	880 J m <sup>-2</sup>	[96]
Recombinant proteins	Lap-shear test	ASTM F2255 (modified), 1 × 1 cm <sup>2</sup>	porcine skin	20 min, wet	0.1341 ± 0.0052 MPa	[96]
	T-peel test	ASTM F2255 (modified)	porcine skin	20 min, wet	≈50 N m <sup>-1</sup>	[96]

(Continued)

**Table 2.** (Continued).

Adhesive system	Method	Test conditions	Substrate	Curing conditions	adhesion strength/ adhesion energy	Ref.
recombinant MAP fp-151	Lap-shear test	ASTM D1002 (modified), 10 × 10 mm <sup>2</sup>	aluminum	3 h, dry, 37 °C	0.8 ± 0.2 MPa	[104]
co-expressed fp-151 + tyrosinase	Lap-shear test	ASTM D1002 (modified), 10 × 10 mm <sup>2</sup>	aluminum	3 h, dry, 37 °C	3.01 ± 0.62 MPa	[105]
fp-151 + hyaluronic acid coacervate	Lap-shear test	1 mm min <sup>-1</sup> , 10 × 10 mm <sup>2</sup>	porcine skin	24 h, 37 °C, humid	0.0572 ± 0.0097 MPa	[106]
recombinant barnacle cement protein rBalc19k	Atomic force microscopy (colloidal probe)	contact time 2 s, 1 μm s <sup>-1</sup>	mica	-	≈3 mN m <sup>-1</sup> ; 0.7 mJ m <sup>-2</sup>	[107]
DOPA-modified recombinant spider silk proteins	Lap-shear test	10 mm min <sup>-1</sup> , 50 × 10 mm <sup>2</sup>	aluminum	24 h, dry	≈1.38–1.58 MPa	[108]
Spider silk-MAP fusion protein	Lap-shear test	10 mm min <sup>-1</sup> , 50 × 10 mm <sup>2</sup>	pig bone	24 h, dry	1.2 to 2.1 MPa	[109]
Amyloid-silk-MAP fusion protein	Surface force apparatus	-	mica	wet	55 mN m <sup>-1</sup> ; 12 mJ m <sup>-2</sup>	[109]
	Lap-shear test	2 mm min <sup>-1</sup> , 10 × 10 mm <sup>2</sup>	porcine skin	18 h, 37 °C, wet	0.078 ± 0.011 MPa	
	Lap-shear test	2 mm min <sup>-1</sup> , 10 × 10 mm <sup>2</sup>	glass	18 h, 37 °C, wet	1.0 ± 0.3 MPa	
	Lap-shear test	2 mm min <sup>-1</sup> , 10 × 10 mm <sup>2</sup>	glass	18 h 37 °C wet, then FeCl <sub>3</sub> solution or buffer pH 11 for 8 h	≈0.3 MPa	
Spider silk-cellulose binding domain fusion protein	Lap-shear test	2 mm min <sup>-1</sup> , 10 × 10 mm <sup>2</sup>	aluminum	18 h 37 °C wet, then FeCl <sub>3</sub> solution or buffer pH 11 for 8 h	0.25 ± 0.158 MPa	[110]
<i>de novo</i> repetitive peptides/sodium dodecylbenzene sulfonate (SDBS) coacervate	Lap-shear test	5 μm s <sup>-1</sup> , 10 × 10 mm <sup>2</sup>	bacterial cellulose	10 min, 50% RH	75 N cm <sup>-2</sup>	[111]
	Lap-shear test	10 mm min <sup>-1</sup> or 40 mm min <sup>-1</sup> , 5 × 5 mm <sup>2</sup>	glass, steel	12 h, dry	11.0 to 14.0 MPa	
	Lap-shear test	10 mm min <sup>-1</sup> or 40 mm min <sup>-1</sup> , 5 × 5 mm <sup>2</sup>	aluminum	12 h, dry	0.33 MPa, 0.49 MPa	
<i>de novo</i> repetitive peptides/negatively charged DOPA-surfactant + Fe <sup>3+</sup>	Lap-shear test	10 mm min <sup>-1</sup> or 40 mm min <sup>-1</sup> , 5 × 5 mm <sup>2</sup>	steel	12 h dry, then 1 h wet	13.5 ± 1.6 MPa	[97]
	Lap-shear test	10 mm min <sup>-1</sup> or 40 mm min <sup>-1</sup> , 5 × 5 mm <sup>2</sup>	steel	12 h, dry	≈16 MPa	
<i>de novo</i> repetitive peptides/negatively charged azobenzene-surfactant	Lap-shear test	10 mm min <sup>-1</sup> or 40 mm min <sup>-1</sup> , 5 × 5 mm <sup>2</sup>	steel, glass	30 min dry, then wet overnight	≈0.4 ± 0.07 MPa, ≈0.36 ± 0.08 MPa	[112]
<i>de novo</i> repetitive peptides/DNA coacervates	Lap-shear test	10 mm min <sup>-1</sup>	glass, steel, Cu, ceramics	10 h, dry	15.4 to 21.3 MPa	[113]
<i>de novo</i> repetitive peptides/crown ether coacervates	Lap-shear test	50 mm min <sup>-1</sup>	porcine skin	10 h, dry	17.2 ± 13.0 J m <sup>-2</sup>	[114]
<i>de novo</i> repetitive peptides/SDBS coacervate + gold nanorods	Lap-shear test	10 mm min <sup>-1</sup> , 3 × 5 mm <sup>2</sup>	steel	5 days, 33 °C, dry	22.3 ± 2.1 MPa	
	Lap-shear test	10 mm min <sup>-1</sup> , 3 × 5 mm <sup>2</sup>	glass, steel, aluminum	4 days, dry	13.0 to 20.0 MPa	
	Lap-shear test	10 mm min <sup>-1</sup> , 3.5 × 9 mm <sup>2</sup>	porcine skin	1 h, dry	0.015 ± 0.0025 MPa	
	Lap-shear test	10 mm min <sup>-1</sup> , 3.5 × 9 mm <sup>2</sup>	porcine skin	808 nm irradiation, 30 s intervals	≈0.065 MPa	

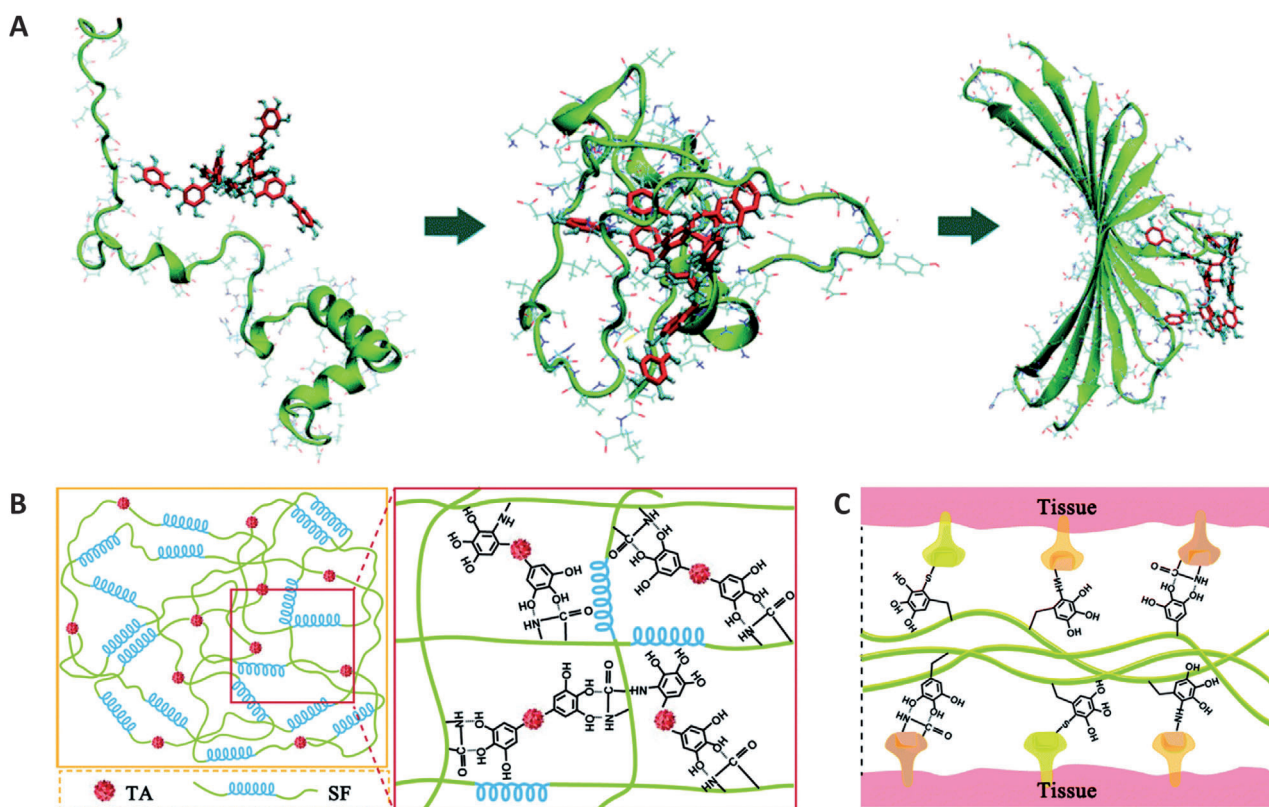


**Figure 7.** Bio-inspired adhesive comprising catechol-modified silk fibroin. A) Molecular dynamics simulations support the hypothesis of the impact of tannic acid (red) on the conformational transition of the silk protein (green) into a  $\beta$ -sheet-rich fold. B) Schematic representation of the hierarchically assembled nanofibrillar structure, responsible for the cohesion properties. C) Proposed schematic adhesion mechanism on tissue through binding to nucleophilic surface molecules. Reproduced (Adapted) with permission.<sup>[96]</sup> Copyright 2016, Royal Society of Chemistry.

Even more powerful adhesion can be obtained by combining two or more adhesion mechanisms. In a recent study, Bashir et al. reported a glue with wet adhesion based on chemical DOPA modification of one component and cohesion promoted by liquid-liquid phase separation.<sup>[103]</sup> The use of  $\beta$ -lactoglobulin and oppositely charged DOPA-functionalized pectin led to formation of a coacervate, which was assumed injectable through a syringe without clogging due to shear-thinning behavior. Adhesive strength was determined to a maximum of 1.5 MPa in lap-shear tests using porcine skin, and after 1 min an adhesion of already 0.27 MPa was measured. The rise in adhesive strength within several hours is a generally commonly observed phenomenon, which could be attributed to the slow curing process via DOPA-quinone oxidation and crosslinking. However, a rapid increase in adhesive strength up to 134 kPa within 20 min has been observed by Bai et al.<sup>[96]</sup> Instead of DOPA, the group reached back to tannic acid (TA), a natural polyphenol that can be extracted from plants. TA contains five catechol groups and has a high affinity to nucleophiles (like amines and thiols), thus interacting with the amino acids of silk fibroin. The addition of TA to an aqueous silk fibroin solution induced the conformational transition from initially mostly random coil to mainly  $\beta$ -sheet (Figure 7A). The experimental observations were supported by molecular dynamics simulations, which suggested strong hydrogen bonds between

TA and hydroxyl or amino groups of the protein upon mixing, followed by  $\pi$ - $\pi$ -stacking interactions as the folding proceeds. This co-assembly of silk and TA led to spontaneous gelation, or in other words, to the formation of a nanofibrillar structure, which resulted in improved toughness (Figure 7B). Wet adhesion (in water and blood) was confirmed on substrates like porcine skin and exceeded the adhesion strength of other clinically used adhesives like cyanoacrylate or fibrin glue. The tannic acid was explained to strongly interact with nucleophilic molecules displayed on the tissue surface (Figure 7C). Sealing effects and good cytocompatibility were demonstrated in vivo in rat model hearts and intestines, and the silk glue showed hemostatic ability as well as antibacterial effects. Furthermore, 45 days after application, the glue was degraded to 80% and replaced by the rat's own cells.

## 3.2. Recombinant Adhesive Proteins

### 3.2.1. Natural-Like Designed Adhesive Proteins

With the technology of genetic engineering and protein design, new bioadhesives can be generated in high purity and consistent quality along with good manufacturing practice (GMP) standards, ensuring also biological safety for in vivo applications. On

the basis of natural Mfps, a multitude of recombinant MAPs were created, like the recombinant hybrid MAP called fp-151, which combines the sequences of Mfp-1 and Mfp-5 (Figure 8).<sup>[116]</sup> This particular recombinant protein is a good example of the manifold possibilities related to genetic engineering. Starting with a recombinant natural-like Mfp-5, difficulties such as low yields and low solubility in aqueous buffers became apparent along with protein production in *E. coli* and purification.<sup>[116]</sup> These limitations were overcome by design of the hybrid protein, fusing Mfp-5 with Mfp-1-derived decapeptide repeats at the termini. The strategy for bacterial expression and purification was moreover optimized toward biosafety, obtaining an endotoxin-free and safe product.<sup>[117]</sup> One remaining challenge was the incorporation of the non-canonical amino acid DOPA into recombinant MAP, due to the expression host lacking the post-translational modification system of mussels. It can be achieved either by *in vitro* modification of tyrosine residues using tyrosinase enzymatic treatment after or during protein purification, or *in vivo* during protein translation. Through co-expression of fp-151 with a recombinant tyrosinase in *E. coli* for *in vivo* DOPA modification, the group of Cha detected a 4-fold increased adhesive strength (3 MPa) compared to that of the same protein modified *in vitro* (0.8 MPa).<sup>[104]</sup> This was explained by increased protein solubility and better exposure of tyrosine residues. However, this pathway represents an additional effort compared to conventional modifications by commercially available mushroom tyrosinase and produced mainly the oxidized DOPA-quinone. A simpler *in vivo* modification method uses the endogenous tyrosyl-tRNA synthetase (TyrRS) of the expression host. The strategy is based on the binding affinity for DOPA being competitive with that for tyrosine. Supplemented DOPA is loaded to the tRNA intended for tyrosine as soon as no tyrosine is available in respective auxotrophic cells and is residue-specifically incorporated with a detected yield of >90% of tyrosine residues.<sup>[118]</sup> To further improve cell-interaction with the bioadhesive, a version of fp-151 with the cellular recognition motif RGD was generated and demonstrated to be suitable for tissue engineering.<sup>[119]</sup> A more recent study describes a complex coacervate glue using the cationic fp-151 and negatively charged hyaluronic acid, a component of the extracellular matrix.<sup>[105]</sup> After *in vitro* DOPA modification, the coacervate was loaded with two drugs, epidermal growth factor, and allantoin, and was applied through a syringe to fix autologous skin grafts in place. The drug-loaded coacervate exhibited a wet adhesion strength of 57 kPa and, compared to fibrin glue (25 kPa) and black silk suture threads, promoted faster *in vivo* wound regeneration with less scarring and inflammatory response, caused by the steady release of the drugs.

Several other recombinant adhesive proteins, which are natural-like by design, have been reported to date. For a comprehensive overview of recombinant Mfps, we would like to refer to Wang and Scheibel (2018).<sup>[120]</sup> Nevertheless, a recombinant Mfp-6-based protein is worth noting, as it is able to rescue DOPA activity after oxidation to DOPA-quinone.<sup>[121]</sup> Considering other natural-like engineered proteins besides the mussel as a model, a recombinant barnacle cement protein rBalcp19k was reported, which self-assembled into nanofibers at acidic and low-ionic conditions.<sup>[106]</sup> Fibrillar structures were highly stable and showed a lower adhesion capacity than a commercial DOPA-based adhesive, but also less pH-dependent decline in adhe-

sion, proposing a more robust adhesion mechanism than the DOPA-based one. Li et al. demonstrated recombinant spider aggregate glue proteins (AgSp1), which allowed biomimetic wet spinning into fibers. Structure and mechanical properties were analyzed, but no data on adhesive properties were shown.<sup>[122]</sup> Some recombinant spider silk materials possess antimicrobial or microbe-repellent properties, and are biocompatible, degradable, and non-immunogenic, thus representing a predestined material for biomedical applications.<sup>[123]</sup> Further, some silks display intrinsic adhesive properties.<sup>[123–124]</sup> Two recombinant spider silk proteins were demonstrated recently by Bogush et al. to possess good wettability and adhesive strength on organic and inorganic substrates.<sup>[107]</sup> Differences in breaking shear stress between both proteins were attributed to the different proline content, as proline with its pyrrolidine ring introduces steric constraints into the protein backbone, disturbs the crystalline  $\beta$ -sheet regions and induces  $\beta$ -turns, which generally contributes to a higher elasticity of silk.<sup>[125]</sup> Adhesion was furthermore observed during lap-shear experiments to be higher in a wet environment, and breaking of the adhesive bond was caused by cohesive failure of the material. The group then compared these results to the performance of their proteins after *in vitro* DOPA modification using a recombinant tyrosinase. The enzymatic tyrosine-to-DOPA conversion with a maximum yield of 57% of total tyrosine residues was not complete, but could not be further increased. Nevertheless, it led to an increase in the protein adhesion capacity by 26–75%.

### 3.2.2. Chimeric/Hybrid Fusion Adhesive Proteins

The intermediate level of tyrosine residues in for example spider silk (3–4%)<sup>[107]</sup> can be increased by genetic engineering for DOPA-based adhesion. Aich et al. designed a fusion protein between a mussel foot protein motif (Mfp-3) and a spider dragline silk protein (Figure 8).<sup>[108]</sup> After recombinant expression, the fusion protein's tyrosine residues were in part enzymatically converted into DOPA by tyrosinase during the purification process yielding 20% of conversion. More precisely, modification was performed on the resin-bound Hexa-histidine tagged protein during immobilized metal ion affinity chromatography (IMAC), simplifying the subsequent removal of the enzyme. Structural analysis of the fusion protein showed the ability to self-assemble into fibrils, leading to the suggestion that the silk portion determines the protein structure, and fibril assembly was not hindered by the additional MAP sequence. This might be advantageous for an adhesive since reduced cohesion and adhesion stresses have been suggested in highly flexible self-assembled fibrillar structures, caused by a more effective dissipation of energy across the protein molecules. Moreover, the fibrillar assembly enlarges the surface area of the material, enabling a higher degree of adhesive interactions in contact with the substrate.<sup>[13]</sup> The MAP portion, in turn, contributes significantly to wet surface adhesion, illustrated by the detected 3-fold higher surface adhesion energy of the fusion protein compared to the pure silk without DOPA modification (Figure 9).

The benefit of a nanofibrillar structure is also evident when analyzing amyloid-like proteins. A silk-amyloid-Mfp hybrid protein was generated by Kim et al. by alternatingly combining sequences from a domain of the A $\beta$ -amyloid protein, which

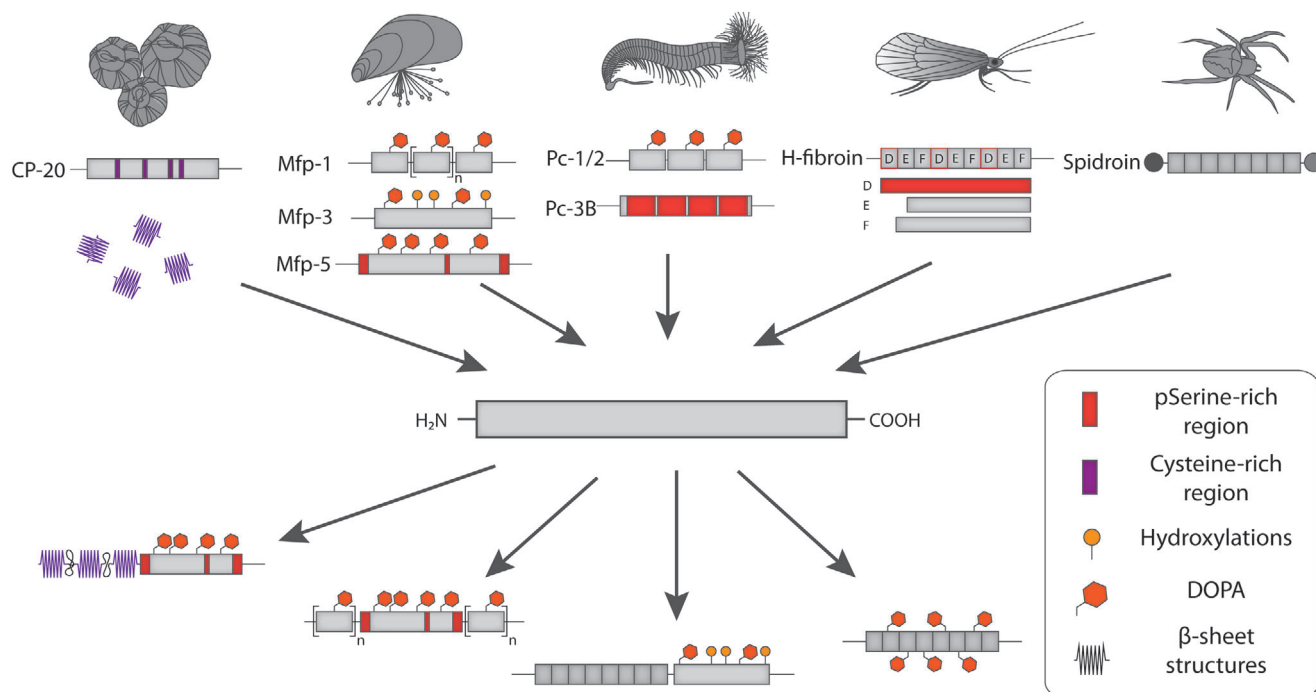


**Figure 8.** Recombinant engineering enables the combination of different natural motifs or domains (upper part) into new adhesive proteins (lower part).

tends to self-assemble into crystalline  $\beta$ -sheets, with the flexible glycine-rich region of a MaSp1 spider silk protein.<sup>[109]</sup> A mussel foot protein (Mfp-5) was added at the C-terminus of the 8-fold repetitive sequence (Figure 8). The group used a tyrosine-auxotrophic *E. coli* strain for protein expression and added DOPA to the culture medium, resulting in the *in vivo* incorporation of DOPA instead of tyrosine residues with 79–86% efficiency. Hydrogels made of the hybrid protein exhibited a high stretchability (up to three times the length), indicating good cohesion caused

by the amyloid-silk moiety, as well as a strong underwater adhesion on various substrates (78 kPa on porcine skin, 1 MPa on glass). Oxidation of DOPA induced by a basic pH or the addition of  $\text{FeCl}_3$  solution for catechol- $\text{Fe}^{3+}$  chelation was observed to reduce the wet adhesive interactions significantly and was proposed to be used for controllable debonding of the adhesive.

Despite *E. coli* being the working horse of recombinant protein production, due to drawbacks of bacterial expression systems like protein aggregation or misfolding when reaching

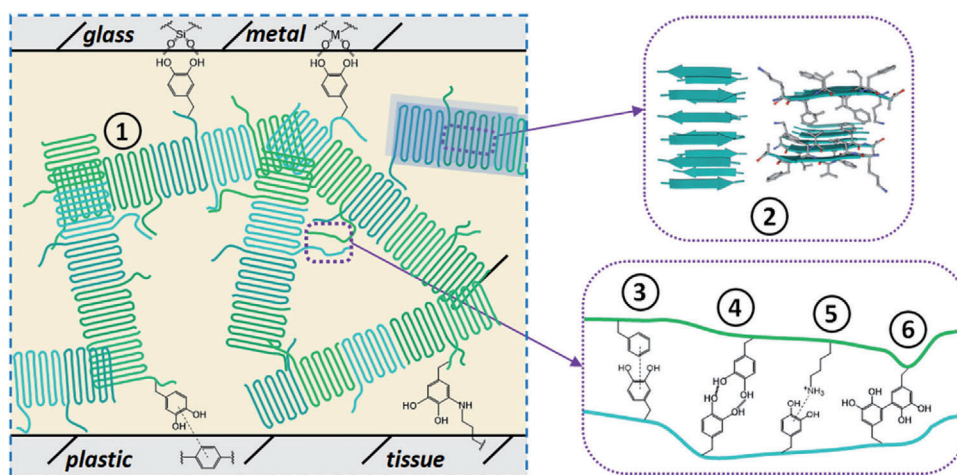


**Figure 9.** Proposed adhesive and cohesive interactions of hybrids combining structural proteins, like amyloids or spidroins, with DOPA-containing proteins. Adhesion results from bidentate hydrogen bonding with metal oxide surfaces as well as  $\pi$ - $\pi$ -stacking on plastic and covalent bonds via Michael-type addition with lysines or cysteines within a tissue. Cohesive interactions include 1) intermolecular hydrogen bonds, 2) interactions between parallel  $\beta$ -sheets, 3)  $\pi$ - $\pi$ -stacking, 4) bidentate hydrogen bonding, 5) cation- $\pi$  interactions, and 6) covalent bonds between two DOPA groups via aryloxyl radicalization. Reproduced (Adapted) with permission.<sup>[109]</sup> Copyright 2021, American Chemical Society.

high expression levels and the limitations in post-translational modifications,<sup>[126]</sup> first efforts were made to switch to eukaryotic expression hosts for new bio-inspired adhesives.<sup>[127]</sup> Two chimeric Mfp-amyloid proteins combining Mfp-3 with amyloid-forming gas vesicle protein A (GvpA) from a cyanobacterium, as well as Mfp-5 with the *E coli* curli protein CsgA, were produced in the yeast *P. pastoris*.<sup>[127b]</sup> Adhesion in a wet environment was improved in both cases upon addition of the amyloid moiety.

Lastly, spontaneous simple coacervation was the inspiration of choice for the design of a recombinant hybrid protein, comprising a spider silk repetitive core domain engineered with terminal cellulose binding domains.<sup>[110]</sup> The block-architecture of intrinsically disordered silk domains and the folded, thermally stable terminal domains led to self-coacervation at high concentrations and low ionic strength. The coacervate displayed increased adhesion on several cellulose-based materials like paper, bacterial cellulose, cotton, and wood.

### 3.2.3. De Novo Designed Adhesive Proteins

The emerging field of de novo protein design has also reached biomaterials research, reflected in the recently presented de novo protein adhesives inspired by coacervation.<sup>[111–112]</sup> Imitating a very short elastin-like polypeptide sequence, positively charged repetitive proteins with various lengths were constructed ((VPGXG)<sub>n</sub>, X = cationic amino acid). Mixing with salmon sperm DNA or sodium dodecylbenzene sulfonate (SDBS) as negative counterparts yielded complex coacervates with a high lap-shear strength (up to 21.3 MPa, dry conditions) comparable to cyanoacrylate superglues, depending on polymer length and type of positive charge. Stronger adhesion was detected in case of proteins with a higher number of repetitions, and when the positively charged amino acid was arginine instead of lysine, stronger cation- $\pi$  interactions were gained. In addition, the coacervate including the DNA exhibited a more robust interfacial adhesion, probably due to  $\pi$ - $\pi$ , cation- $\pi$ , and hydrogen bonding provided by the nucleobases. Adhesive properties could even be more increased by the combination of the repetitive proteins with other negatively charged molecules like crown-ether, which introduce additional host-guest interactions through their ring-like structure and result in a strong adhesive withstanding also extreme temperature conditions.<sup>[113]</sup> Moreover, as negative counterparts synthetic surfactants containing DOPA or aromatic-rich azobenzene moieties were tested, also resulting in high adhesion strength due to additional DOPA-mediated or  $\pi$ - $\pi$  stacking and cation- $\pi$  interactions.<sup>[97]</sup> Combining two natural adhesion motifs, the DOPA-containing coacervate adhesion could be reinforced by the chelation of metal ions through hydroxyl groups and was found also functioning in wet conditions. The coacervate glues were found biocompatible (90% cell viability after 24 h), biodegradable, antibacterial, and showed reduced inflammatory responses.<sup>[112]</sup> Therefore, it was suggested suitable for biomedical applications including wound closure devices and tissue regeneration set-ups. One proposed possible application was demonstrated to be photothermal therapy for skin tumors like melanoma, enabling a non-invasive strategy with an adhesive bioplastic.<sup>[114]</sup> The adhesive coacervate was designed with cysteine residues at the ter-

mini of proteins, allowing complexation with gold nanorods via gold-sulfur bonds. Because gold nanorods strongly absorb near-infrared light, the resulting heating of the patch upon laser irradiation leads to protein denaturation, DNA breakage, and ultimately death of adjacent cancer cells, demonstrated in vivo by inhibition of tumor growth paired with improved wound healing and skin regeneration. The adhesion of the coacervate was not affected by the modification; in fact, adhesion strength increased with longer curing time and after short laser irradiation, probably caused by the photothermal effect leading to accelerated evaporation of water and therefore strengthening molecular interactions. Although the de novo design of protein-based adhesives is still in its infancy, this strategy represents a promising approach for the future to generate tailor-made biomaterials.

## 4. Activatable Adhesives

Extending the application of an adhesive toward usage inside a human body comes with several challenges. While with external wounds, depending on the site of application, an adhesive has to withstand motion-induced shear forces, the treatment of internal wounds additionally presents a dynamic, wet environment often accompanied by the presence of blood. This can result in undesired pre-mature polymerization or reactions limiting the adhesive strength. Further, rearrangement of misplaced adhesive patches is practically only possible with activatable surfaces or adhesives.<sup>[128]</sup> The following discusses some of the currently studied activatable wound sealing and adhesive systems to overcome these challenges (Table 3).

### 4.1. Photo-Activation to Induce Adhesion

The curing of polymer adhesives is an important aspect toward a triggerable mode of action and can be defined as the induced polymerization using a catalytic or co-reactive agent, which is also termed hardening.<sup>[142]</sup> A widely applied mechanism for adhesion activation described in literature is photo-curing with or without the use of photo-initiators due to convenient and efficient spatiotemporal activation control.<sup>[143]</sup> Methacrylic-group functionalized polymers account for the most prominent examples found in literature. However, among protein-based adhesives, the canonical amino acid tyrosine has a particularly intriguing potential as it can be either used to introduce catechol groups through enzymatic hydroxylation or used in its natural state to form di-tyrosine bonds through photo-oxidative reactions. Especially the use of white-light photo-initiator systems employing ruthenium complexes in combination with an electron acceptor such as sodium persulfate presents a promising strategy to form tyrosyl radicals, which then react with other proximate tyrosine residues of either the adhesive protein or the ones presented by the tissue surface, hence, increasing the adhesive strength.<sup>[144]</sup> The use of visible-light curable systems circumvents issues concerning secondary damage through UV-light traditionally used in photo-activatable materials. Recombinant MAPs make a substantial contribution in this particular niche, as they contain a high mole percentage of tyrosine residues.

**Table 3.** Selection of activatable protein and protein-based adhesives.

Mechanism	Composition	Activation time	Test method	Substrate	Adhesion strength/ adhesion energy	Proposed application	in vivo studies	Ref.
<b>Light</b>								
radical polymerization	AlgMA + GelMA	4 min UV, 30 min CaCl <sub>2</sub>	Tensile test, 10 mm min <sup>-1</sup>	porcine ureter	≈0.09 MPa (wet)	sealant	No	[9]
dityrosine cross-linking, photo-oxidation via Ru(II)(bpy <sup>2+</sup> ) <sub>3</sub> ; λ = 452 nm	recombinant MAP ("LAMBA")	1 min	Lap-shear-test, 100 mm <sup>2</sup> , 5 mm min <sup>-1</sup> (10kN)	porcine skin	0.048 ± 0.01 MPa (wet)	various (e.g. brain, liver, breast)	Yes	[129]
dityrosine cross-linking, photo-oxidation via Ru(II)(bpy <sup>2+</sup> ) <sub>3</sub> ; λ = 460 nm	MAP-Substance P fusion protein	1 min	Lap-shear-test	porcine skin	0.042 ± 0.001 MPa (wet)	hemostatic, peripheral nerve injuries	Yes	[130]
dityrosine cross-linking, photo-oxidation via Ru(II)(bpy <sup>2+</sup> ) <sub>3</sub> ; λ = 460 nm	recombinant MAP ("FixLight")	1 min	Lap-shear-test, 100 mm <sup>2</sup> , 1.2 mm min <sup>-1</sup> (10kN)	porcine scleral tissue	0.028 ± 0.002 MPa (wet)	tissue grafting (e.g. amniotic membrane transplantation)	Yes	[131]
cleavage of restrictive ortho-nitrobenzyl (ONB) group; λ = 365 nm	recombinant MAP containing non-canonical ONB-DOPA	45 min	Atomic force microscopy	mica	-	prove of principle	No	[132]
radical polymerization	poly(glycerol sebacate acrylate) (PGSA)	0.5 min	Pull-off adhesion test (90°), 8 mm min <sup>-1</sup>	porcine epicardial tissue	≈ 2 N cm <sup>-2</sup> (wet)	hemostatic, treatment of e.g. ventricular and vascular defects	Yes	[128]
radical polymerization	GelMA + hemocoagulase	4 min	Lap-shear-test, 1 mm/ min	glass	0.093 ± 0.009 MPa (dry)	hemostatic, treatment of strong bleeding wounds	Yes	[133]
		4 min	End-to-end joint tensile test, 300 mm <sup>2</sup> , 1 mm/ min	porcine skin	0.035 ± 0.003 MPa (wet)			
<b>Temperature</b>								
thermal phase-transition, coacervation	DOPA-modified elastin-like protein (ELY <sub>16</sub> )	24 h at 37 °C	Lap-shear-test, 2 mm min <sup>-1</sup> (2kN)	aluminum	0.24 ± 0.09 MPa (wet)	not specified	No	[134]
thermal phase-transition, coacervation	elastin-like protein + sodium dodecyl benzene sulfonate (SDBS)	30 min at 37 °C/ 4 °C	Lap-shear-test, 25mm <sup>2</sup> , 10 mm min <sup>-1</sup>	glass/ PVC	0.5 – 0.6 MPa (wet)	not specified	No	[135]
		30 min at 37 °C/ 4 °C	Lap-shear-test, 84 mm <sup>2</sup> , 50, and 200 mm min <sup>-1</sup>	porcine skin	≈0.008 MPa (wet)			
thermal phase-transition, coacervation	MAP-PNIPAM conjugate + decellularized adipose tissue	5 min at 37 °C	Pull-off adhesion test (90°), 0.3 mm min <sup>-1</sup>	porcine skin	≈0.006 MPa (wet)	adipose tissue	Yes	[136]
dynamic Schiff base bonds	Gelatine and chondroitin sulfate aldehyde + borax	20 min at 37 °C/ 20 °C	Lap-shear-test, 100 mm <sup>2</sup> , 1 mm min <sup>-1</sup>	porcine skin	≈0.03 MPa (wet)	hemostatic, various	Yes	[137]

(Continued)

**Table 3.** (Continued).

Mechanism	Composition	Activation time	Test method	Substrate	Adhesion strength/ adhesion energy	Proposed application	in vivo studies	Ref.
<i>pH</i>								
controlled $\beta$ -sheet formation via despi switch defects	recombinant MAP/ mfp	pH 5.5 to pH 6.8	Atomic force microscopy	silica	$2.64 \pm 0.15 \text{ mJ m}^{-2}$ (wet)	prove of principle	No	[138]
controlled oxidation by network-bound boronic acid	dopamine methacry- lamide and 3-acrylamido phenylboronic acid	pH 3 to pH 9	Atomic force microscopy	borosilicate glass	$\approx 2 \text{ J m}^{-2}$ (pH 3) (wet)	prove of principle		[139]
<i>Chemical</i>								
induced oxidation	hyaluronic acid prepolymers with either catechol or NCSN group	instant	Lap-shear-test, 6.25 mm <sup>2</sup> , 1 mm min <sup>-1</sup>	glass	$\approx 0.04 \text{ MPa}$ (dry)	gastric tissue	Yes	[140]
		instant	Lap-shear-test, 6.25 mm <sup>2</sup> , 1 mm min <sup>-1</sup>	glass	$\approx 0.015 \text{ MPa}$ (wet)			
<i>Contact</i>								
absorbance of interfacial water	PAAc-NHS ester cross-linked with GelMA + gelatine	5 s	Tensile test, 6.25 mm <sup>2</sup> , 50 mm min <sup>-1</sup> (2.5 kN)	various tissues	0.02 – 0.12 MPa (wet)	skin, small intestine, stomach, muscle, heart, and liver	Yes	[141]
		5 s	Pull-off adhesion test (90°/180°), 50 mm min <sup>-1</sup>	various tissues	190 – 700 J m <sup>-2</sup> (wet)	skin, small intestine, stomach, muscle, heart, and liver		

Jeon et al. described a light-activated, mussel protein-based bioadhesive (LAMBA) (Figure 10A), which could be cured within 60 s and exhibited wet-adhesive strength higher than that of common fibrin-glues ( $\approx 50$  kPa). LAMBA further showed rapid re-epithelialization and significantly faster reduction in wound areas in rats compared to cyanoacrylate-based glues.<sup>[129]</sup> More recently, Cheong et al. extended this approach and described the development of a MAP-based hydrogel, activated by visible-light and genetically fused with the neurotransmitter Substance P (MAP-SP) for sutureless neurorrhaphy (Figure 10B). SP was reasoned to mediate polarization of macrophage subtypes, which are involved in the transition between the inflammatory response and repair/remodeling phase of nerves. While neurorrhaphy with sutures can inflict traumatic damage and severe inflammation around the injured nerve tissues, MAP-SP exhibited good wet-adhesion and induced genotypic and phenotypic characteristic M2 macrophage polarization promoting functional nerve regeneration.<sup>[130]</sup> Maeng et al. developed a MAP-based adhesive termed FixLight with proposed application for effective sutureless amniotic membrane transplantation (AMT) (Figure 10C). The amniotic membrane is a tissue derived from the placenta and has attracted attention as a promising material for use in tissue regeneration since it modulates adult wound healing by suppressing stromal inflammation, angiogenesis, and scarring while promoting epithelialization.<sup>[145]</sup> However, this approach still requires suturing to attach the membrane. In this regard, FixLight could be used to rapidly perform AMT in rabbit conjunctiva defect models compared to time-consuming suturing

and showed a wet adhesive strength of  $\approx 28$  kPa comparable to common fibrin glues.<sup>[131]</sup> Further underlining the utility of recombinant protein-based adhesives, an intriguing study by Hauf et al. describes the development of a photocaged DOPA-derivative termed ortho-nitrobenzyl DOPA (ONB-DOPA), which could be incorporated into MAPs through an engineered *M. jannaschii* tyrosyl-tRNA synthetase (MjTyrRS).<sup>[132]</sup> Using engineered aminoacyl-tRNA synthetases (aaRS), site-specific incorporation of non-canonical amino acids such as ONB-DOPA can be performed in living cells with higher specificity and yields. The ONB group is then cleaved upon irradiation ( $\lambda = 365$  nm) allowing for spatiotemporal control of the adhesive catechol side chains (Figure 10D). However, this method only achieved >50% deprotection upon irradiation for 45 minutes, making it rather unpractical for surgical use at this stage.

While purely natural adhesives exhibit limitations in adhesive strength and toughness, and purely synthetic adhesives raise concerns regarding toxic degradation products, attention has been directed toward semisynthetic multifunctional systems. For example, a hybrid system combining methacrylate-modified alginate (AlgMA) and gelatin-methacryloyl (GelMA) has been developed by Tavafoghi et al., which could be applied to a wound and cross-linked by two mechanisms. The first cross-linking occurred under visible-light by the reaction of methacrylate and methacryloyl-groups followed by metal ion-induced physical cross-linking of mannuronic- and guluronic-acid blocks present in the alginate compound. While the chemically cross-linked MA-groups of GelMA and AlgMA maintained

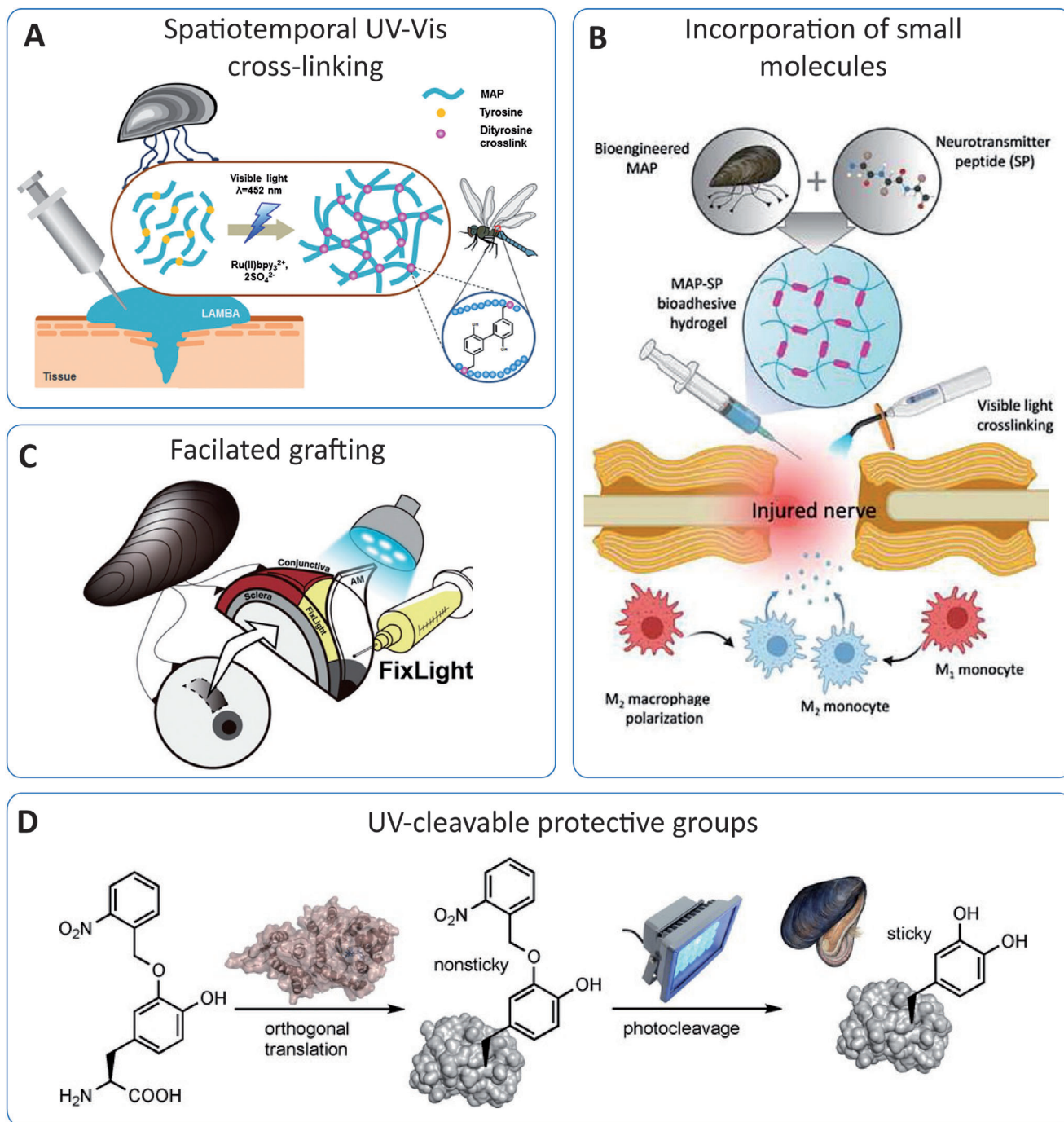


**Figure 10.** Examples of photo-activatable protein-based adhesive systems and their advantages in surgery. A) Di-tyrosine crosslinking can be induced by UV-vis light irradiation in tyrosine-rich proteins such as MAPs. This approach resembles the mechanism found in insects. Reproduced with permission.<sup>[129]</sup> Copyright 2015, Elsevier. B) Incorporation of small molecules such as neurotransmitters into bio-inspired protein-glue systems enables rapid and sutureless neurorrhaphy of sensible tissue such as nerves, in which macrophage-polarizing properties improve regeneration. Reproduced with permission.<sup>[130]</sup> Copyright 2022, Elsevier. C) Rapid light-induced polymerization allows relatively easy and quick transplantation of regenerative tissue grafts, for instance, the amniotic membrane, to otherwise difficult-to-operate organs such as the eye. Reproduced with permission.<sup>[131]</sup> Copyright 2021, Wiley-VCH GmbH. D) A more elaborate route for photo-activation is the use of protective groups such as photocaged ortho-nitrobenzyl (ONB)-DOPA, a non-canonical amino acid that is introduced into the amino acid sequence upon recombinant production using engineered tRNA synthetases. The DOPA group is deprotected upon exposure to UV light. Reproduced with permission.<sup>[132]</sup> Copyright 2017, Wiley-VCH GmbH.

structural integrity, the physical crosslinking provided a polymer network that dissipated energy under stress.<sup>[9]</sup> However, the reactivity with blood was not shown in this study and is a considerable drawback. To encounter this issue, materials with hemostatic properties are of great interest. For example, Lang et al. describe a hydrophobic UV-light-activated adhesive (HLAA) composed of poly(glycerol sebacate acrylate) (PGSA) tested in small and large animal models. The hydrophobic character prevented washing-off and retained its adhesive strength even after prolonged contact with blood. Therefore, the adhesive was able to effectively seal left ventricular wall defects in rats for as long as 180 days.<sup>[128]</sup> Taking photo-activatable, hemostatic systems to another level, a study presented by Guo et al. used hemocoagulase derived from snake venom together with GelMA to develop a material that could rapidly seal bleeding wounds within seconds of application and subsequent curing for the potential treatment of heavily bleeding wounds.<sup>[133]</sup>

#### 4.2. Temperature-Activation to Induce Adhesion

Another accessible path for adhesion activation is temperature, naturally emitted by the body or possibly also applied externally. Elastin and elastin-like proteins (ELP) harbor a particularly interesting characteristic in this regard, as they show a temperature-dependent inverse phase transition, meaning that these proteins are rendered into a higher ordered state upon increasing temperature and vice versa, readily forming coacervates.<sup>[146]</sup> ELP-based hydrogels with thermo-responsive behavior have been created with tunable lower critical solution temperature (LCST) and have been used, for example, in drug and gene delivery applications.<sup>[147]</sup> Brennan et al. developed an ELP adhesive, in which tyrosine residues were enzymatically converted to DOPA to enable tunable LCST and, hence, reversible coacervation allowing moderate adhesion in humid environments.<sup>[134]</sup> Further, the above-discussed de novo-designed repetitive ELP-like proteins able to form adhesive coacervates with the anionic surfactant sodium dodecyl benzene sulfonate (SDBS) were modified to further incorporate a temperature-dependent adhesive behavior. Upon addition of the repetitive module VPGVG to the sequence consisting of repetitions of VPGKG, phase transition was observed at temperatures above 25 °C, which was accompanied by switching the adhesion strength from ≈600 kPa to a 10-fold decrease.<sup>[135]</sup>

Another strategy is the conjugation of proteins with synthetic thermo-responsive polymers such as poly(*N*-isopropylacrylamide) (PNIPAM) or Pluronic.<sup>[148]</sup> For instance, MAP can be grafted with low molecular weight thermo-responsive PNIPAM (MAP-PNIPAM) through EDC/NHS chemistry as described by Jeon et al., forming gels with LCST ≈30 °C, depending on the degree of grafted PNIPAM, displaying an adhesive strength of ≈6 kPa.<sup>[136]</sup> A hydrogel developed by Zhou et al. consisting of gelatin and aldehyde-functionalized chondroitin sulfate (CS) in the presence of borax allowed dynamic Schiff base bonds enabling a reversible adhesion with higher adhesive strength.<sup>[137]</sup> The injectable and self-healing hydrogel underwent rapid and repeated gel-transition when switching between 37 °C and 20 °C. An adhesive strength of up to ≈30 kPa was reached withstanding up to 800% strain when

using formulations with high gelatin content and CS with a high degree of oxidation. Remarkably, a misplaced adhesive gel could be detached by simply applying cold water and the position readjusted in vivo, further also showing hemostatic properties underlining the utility of such systems.

#### 4.3. pH-Activation to Induce Adhesion

Although mostly underrepresented among protein-based systems, possibly due to the sensitivity of these to pH in regard to protein structure and solubility, pH-induced adhesion has also been described in literature for highly specific applications such as the treatment of gastric wounds.<sup>[149]</sup> The pH could be used to alter the cohesive forces in recombinant MAPs as demonstrated by Arias and colleagues, showing a significant change in adhesive energy when switching from pH 5.5 to pH 6.8. This was hypothesized to relate to suppressed  $\beta$ -sheet formation, which was then facilitated by O→N-acyl transfer rearrangement taking place when shifting toward a more neutral pH.<sup>[138]</sup> Furthermore, Krogsgaard et al. for instance utilized the cationic nature of DOPA in DOPA-functionalized polyallylamine in combination with Fe<sup>3+</sup>-ions to produce a self-healing multi-pH responsive hydrogel. The coordination of DOPA per ferrous-ion depends on pH and formed mono-, bis-, and tris-catechol-Fe<sup>3+</sup> complexes with increasing pH exhibiting the highest shear modulus of 7 kPa at ≈pH 9.3. The adhesive capacity was subsequently dropped at higher pH values closer to the pI as the amine groups started to deprotonate and the hydrogel structure collapsed.<sup>[150]</sup> Narkar et al. presented a hydrogel formed by copolymerizing dopamine methacrylamide and 3-acrylamido phenylboronic acid. The network-bound phenylboronic acid formed a pH-dependent, reversible complex with the catechol-groups protecting it against irreversible oxidation and allowing repeated adhesion and detachment at pH 3 and pH 9 respectively.<sup>[139]</sup>

#### 4.4. Other Activation Systems to Induce Adhesion

To conclude the chapter on activatable adhesives, we further provide some selected examples of adhesives, which do not quite fit into the previous classifications but are worth mentioning. As elaborated previously, the oxidation of DOPA to DOPA-quinone significantly reduces adhesiveness, hence, mechanisms to prevent auto-oxidation (e.g. caged-DOPA) have been used to control the function and rely on the triggered release or deprotection. In a similar approach, Xu et al. describe the use of reducing thiourea groups (NCSN, “nitrogen-carbon-sulfur-nitrogen”) to preserve the adhesiveness of DOPA by preparing two HA-based pre-polymers, of which one contained NCSN and the other catechol-groups.<sup>[140]</sup> Upon mixing, the NCSN reduced already oxidized catechol groups preserving and restoring the adhesive properties. However, by then further applying an oxidation agent, such as simply spraying sodium periodate (NaIO<sub>4</sub>) on top, a rapid pH-independent polymerization could be induced in HA-catechol gels within seconds at ratios of NaIO<sub>4</sub>:catechol 10-times lower than without HA-NCSN. The gels formed by this method exhibited a wet adhesive strength of ≈15 kPa even after incubation in aqueous environments for 24 h and were shown to

promote ulcer healing, enhanced neovascularization, and inflammatory suppression in a porcine model. Thus, the adhesive was proposed as suitable for gastric tissue treatments due to the pH-independent mode of action.

While interfacial water has been established to be a critical factor for adhesion, a study presented by Yuk et al. used poly(acrylic acid) grafted with N-hydroxysuccinimide ester (PAAc-NHS ester) cross-linked using GelMA in combination with an interchangeable biopolymer (e.g. gelatin or chitosan) to incorporate, rather than displace, the usually unfavorable interfacial water at the application site.<sup>[141]</sup> Applied in form of a so-called dry double-sided tape, the quick hydration and swelling result in drying of the surface due to the negatively charged carboxylic acid groups of PAAc-NHS. Subsequently, covalent bonds can be formed via primary amine groups of the tissue, exhibiting rapid interfacial toughness of more than  $600 \text{ Jm}^{-2}$  within 5 s and a tensile strength of up to 160 kPa.<sup>[141]</sup> The storable dry tape has an extensibility of 16 times its original length and has been successfully used to seal several types of tissue both in vitro and in vivo.

## 5. Conclusion and Future Perspective

Bioadhesives can be a useful tool for wound treatment, as they not only provide an often easier and safer form of connecting tissue but also reduce surgical time. The tunable chemistry and, hence, also mechanical and adhesive properties allow their adjustment to the respective needs and can be adapted to meet the properties of a multitude of different tissues. The use of a bioadhesive can become particularly interesting for fragile tissues such as nerves, which can be prone to trauma caused by suturing. In light of the studies on protein-based adhesives presented here, it also becomes apparent that nature can still teach us some tricks, especially when it comes to the design of adhesives used in wet and dynamic environments, which is a particular challenge in surgical applications. A clear trend toward the use of injectable or patch-like hydrogels is obvious as hydrogels facilitate the handling, reduce application time down to seconds, and can infiltrate cavities, uneven surfaces and tissue, further enhancing the adhesive force by mechanism of mechanical interlocking. Especially hydrogels formed by complex coacervation allow strong wet adhesion by displacing or adsorbing interfacial water, which is a major advantage over common cyanoacrylate adhesives. A good bioadhesive should have an adhesive strength in the range of tens of / several kilopascals depending on the tissue or the site of application. While synthetic adhesives with high adhesive strength often suffer from toxic degradation products and poor biodegradability, bioadhesives made of proteins and polypeptides represent a highly versatile alternative. Foremost, the amino acid sequence of protein-based adhesives naturally contains an abundance of available amine and carboxylic groups, which can be readily functionalized or used for conjugation to expand their function. Especially tyrosine-residues play an outstanding role as they can be directly utilized for enzymatic cross-linking or transformation to catechol-groups resembling the naturally occurring DOPA, which in turn has vast modes of action. Recombinant proteins further can be tailored and optimized by rational design and genetic engineering, hence, an in-depth understanding of mechanisms found in natural protein-based bioadhesives is of high importance for their development. Although purely protein-based

adhesives are still often struggling to reach the rather unmatched adhesive strength of synthetic and semi-synthetic glues, their biocompatible nature and the capacity to biodegrade without the release of toxic components is a major advantage, as it also allows the invasion of body's own cells into the glued site promoting re-epithelialization, neovascularization and rapid, close to seamless wound healing. Adding small molecules, drugs, and factors or activatable features to such materials further extends their range of applicability, making them more complex and versatile, allowing for instance good spatiotemporal control over the mode of action or the body's response. However, when looking at developing activatable protein adhesives there are also downsides apart from weaker adhesives forces. While there is a multitude of photo-activatable systems already successfully employed in small and large animal models in vivo, there are only a few temperature-activatable and even less pH-activatable protein adhesives, which have currently exceeded in vitro or even conceptual experimentation. This is most likely due to the fact that especially pH is a common factor directly related to structure and function among all proteins, hence limiting them to a narrow pH range and specific proteins only. Furthermore, feasible production costs, long-term stability, and shelf-time durability are considerable factors, which can limit recombinant protein adhesives for commercial use.

A novel direction in this research field, possibly resolving many of these issues, is known as engineered living materials,<sup>[151]</sup> which among other topics also covers so-called autonomous living glues, aiming to not only create adhesives that can respond to external factors but also display other hallmark features of life such as cell-environment interactions, autonomy, self-replication and -regeneration to create virtually living materials.<sup>[151]</sup> Herein, a dual-strain-strategy of prokaryotes is employed to produce an adhesive on-demand, e.g. induced by light or the presence of heme/blood,<sup>[152]</sup> by the separate expression of a glue protein in one strain and an adhesion-enhancing protein in another, which only in combination form the adhesive matter.<sup>[151,153]</sup> Using this strategy, the "living glue" by An et al. was demonstrated to perform blood-sensing autonomous repair of a microfluidic device.<sup>[152]</sup> Although the pathogenicity of bacteria strains limits the application in the biomedical field, a transfer of the set-up to non-pathogenic organisms or even mammalian cells could overcome this drawback.

## Acknowledgements

The authors acknowledge the funding from the Deutsche Forschungsgemeinschaft (DFG, German Research Foundation) – project number 326998133 in the framework of the Collaborative Research Centre SFB-TRR225 (funded sub-project: A08 and C01). Support from the Elite Network of Bavaria was also acknowledged.

Open access funding enabled and organized by Projekt DEAL.

## Conflict of Interest

The authors declare no conflict of interest.

## Keywords

amyloids, bioadhesions, biomedical applications, coacervation, DOPA, genetic engineering, silks

Received: March 31, 2023  
Revised: May 17, 2023  
Published online:

- [1] I. Skeist, J. Miron, *Handbook of adhesives*, Springer, Berlin **2012**.
- [2] J. Schields, *Adhesives handbook*, Elsevier Science, Amsterdam **2014**.
- [3] L. Xu, Y. Liu, W. Zhou, D. Yu, *Polymers* **2022**, *14*, 1637.
- [4] A. Bal-Ozturk, B. Cecen, M. Avci-Adali, S. N. Topkaya, E. Alarcin, G. Yasayan, Y. C. Ethan, B. Bulkurcuoglu, A. Akpek, H. Avci, K. Shi, S. R. Shin, S. Hassan, *Nano Today* **2021**, *36*, 101049.
- [5] R. Smeets, N. Tauer, T. Vollkommer, M. Gosau, A. Henningsen, P. Hartjen, L. Früh, T. Beikler, E. K. Stürmer, R. Rutkowski, A. L. Grust, S. Fuest, R. Gaudin, F. Avani, *Int. J. Mol. Sci.* **2022**, *23*, 7687.
- [6] L. P. Bré, Y. Zheng, A. P. Pêgo, W. Wang, *Biomater. Sci.* **2013**, *1*, 239.
- [7] B. Mizrahi, C. F. Stefanescu, C. Yang, M. W. Lawlor, D. Ko, R. Langer, D. S. Kohane, *Acta Biomater.* **2011**, *7*, 3150.
- [8] D. García Cerdá, A. M. Ballester, A. Aliena-Valero, A. Carabén-Redaño, J. M. Lloris, *Surg. Today* **2015**, *45*, 939.
- [9] M. Tavafoghi, A. Sheikhi, R. Tutar, J. Jahangiry, A. Baidya, R. Haghniaz, A. Khademhosseini, *Adv. Healthcare Mater.* **2020**, *9*, 1901722.
- [10] T. Divyani, S. Swapna, S. Onkar, *Allied Market Research* **2022**.
- [11] a) S. Khanlari, M. A. Dubé, *Macromol. React. Eng.* **2013**, *7*, 573; b) D. Duchêne, F. Touchard, N. A. Peppas, *Drug Dev. Ind. Pharm.* **1988**, *14*, 283; c) M. L. B. Palacio, B. Bhushan, *Philos. Trans. R. Soc., A* **2012**, *370*, 2321; d) J. Zhu, H. Zhou, E. M. Gerhard, S. Zhang, F. I. Parra Rodríguez, T. Pan, H. Yang, Y. Lin, J. Yang, H. Cheng, *Bioact Mater* **2023**, *19*, 360; e) M. Ramesh, L. R. Kumar, in *Green Adhesives: Preparation, Properties and Applications* (Eds: Inamuddin, R. Boddula, M. I. Ahamed, A. M. Asiri), Scrivener Publishing LLC, Beverly **2020**, 145.
- [12] S. Rathi, R. Saka, A. J. Domb, W. Khan, *Polym. Adv. Technol.* **2019**, *30*, 217.
- [13] Y. Bu, A. Pandit, *Bioact Mater* **2021**, *13*, 105.
- [14] a) N. A. Peppas, P. A. Buri, *J. Controlled Release* **1985**, *2*, 257; b) K. Yoshizawa, H. Murata, H. Tanaka, *Langmuir* **2018**, *34*, 14428.
- [15] T. M. Lutz, C. Kimna, A. Casini, O. Lieleg, *Mater Today Bio* **2022**, *13*, 100203.
- [16] I. D. Whittington, B. W. Cribb, in *Adv. Parasitol.*, Academic Press, New York **2001**, 101.
- [17] M. Kang, K. Sun, M. Seong, I. Hwang, H. Jang, S. Park, G. Choi, S.-H. Lee, J. Kim, H. E. Jeong, *Front. Mech. Eng.* **2021**, *7*, 668262.
- [18] X. Ma, X. Zhou, J. Ding, B. Huang, P. Wang, Y. Zhao, Q. Mu, S. Zhang, C. Ren, W. Xu, *J. Mater. Chem. A* **2022**, *10*, 11823.
- [19] a) J. H. Waite, *J Exp Biol* **2017**, *220*, 517; b) K. Kamino, *Biofouling* **2013**, *29*, 735.
- [20] C. S. Wang, R. J. Stewart, *Biomacromolecules* **2013**, *14*, 1607.
- [21] a) O. Choshesh, B. Bayarmagnai, R. V. Lewis, *Biomacromolecules* **2009**, *10*, 2852; b) M. A. Collin, T. H. Clarke, N. A. Ayoub, C. Y. Hayashi, *Sci. Rep.* **2016**, *6*, 21589; c) V. B. Meyer-Rochow, *Luminescence* **2007**, *22*, 251.
- [22] R. J. Stewart, C. S. Wang, *Biomacromolecules* **2010**, *11*, 969.
- [23] X. Li, S. Li, X. Huang, Y. Chen, J. Cheng, A. Zhan, *Mar. Environ. Res.* **2021**, *170*, 105409.
- [24] a) E. C. Bell, J. M. Gosline, *Mar Ecol Prog Ser* **1997**, *159*, 197; b) S. L. Brazee, E. Carrington, *Biol. Bull.* **2006**, *211*, 263; c) M. W. Denny, B. Gaylord, *Annu. Rev. Mar. Sci.* **2009**, *2*, 89.
- [25] a) J. H. Waite, N. H. Andersen, S. Jewhurst, C. Sun, *J. Adhes.* **2005**, *81*, 297; b) J. H. Waite, H. C. Lichtenegger, G. D. Stucky, P. Hansma, *Biochemistry* **2004**, *43*, 7653.
- [26] K. U. Claussen, T. Scheibel, H.-W. Schmidt, R. Giesa, *Macromol. Mater. Eng.* **2012**, *297*, 938.
- [27] N. R. Martinez Rodriguez, S. Das, Y. Kaufman, J. N. Israelachvili, J. H. Waite, *Biofouling* **2015**, *31*, 221.
- [28] D. G. DeMartini, J. M. Errico, S. Sjoestroem, A. Fenster, J. H. Waite, *J. R. Soc., Interface* **2017**, *14*, 20170151.
- [29] B. P. Lee, P. B. Messersmith, J. N. Israelachvili, J. H. Waite, *Annu. Rev. Mater. Res.* **2011**, *41*, 99.
- [30] a) J. H. Waite, X. Qin, *Biochemistry* **2001**, *40*, 2887; b) R. J. Stewart, T. C. Ransom, V. Hladky, *J. Polym. Sci., Part B: Polym. Phys.* **2011**, *49*, 757.
- [31] H. Lee, N. F. Scherer, P. B. Messersmith, *Proc. Natl. Acad. Sci. U.S.A* **2006**, *103*, 12999.
- [32] J. Saiz-Poseu, J. Mancebo-Aracil, F. Nador, F. Busqué, D. Ruiz-Molina, *Angew. Chem., Int. Ed.* **2019**, *58*, 696.
- [33] Y. Kan, Z. Wei, Q. Tan, Y. Chen, *Sci China Technol Sci* **2020**, *63*, 1675.
- [34] M. J. Sever, J. T. Weisser, J. Monahan, S. Srinivasan, J. J. Wilker, *Angew. Chem., Int. Ed.* **2004**, *43*, 448.
- [35] N. Aldred, L. K. Ista, M. E. Callow, J. A. Callow, G. P. Lopez, A. S. Clare, *J R Soc Interface* **2005**, *3*, 37.
- [36] a) S. Park, S. Kim, Y. Jho, D. S. Hwang, *Langmuir* **2019**, *35*, 16002; b) W. Wei, L. Petrone, Y. Tan, H. Cai, J. N. Israelachvili, A. Miserez, J. H. Waite, *Adv. Funct. Mater.* **2016**, *26*, 3496; c) M. A. Gebbie, W. Wei, A. M. Schrader, T. R. Cristiani, H. A. Dobbs, M. Idso, B. F. Chmelka, J. H. Waite, J. N. Israelachvili, *Nat. Chem.* **2017**, *9*, 473.
- [37] J. Yu, W. Wei, E. Danner, R. K. Ashley, J. N. Israelachvili, J. H. Waite, *Nat. Chem. Biol.* **2011**, *7*, 588.
- [38] L. H. N. Cooper, *J Mar Biol Assoc U K* **1937**, *22*, 167.
- [39] A. H. Hofman, I. A. van Hees, J. Yang, M. Kamperman, *Adv. Mater.* **2018**, *30*, 1704640.
- [40] S. C. T. Nicklisch, J. H. Waite, *Biofouling* **2012**, *28*, 865.
- [41] Q. Lu, E. Danner, J. H. Waite, J. N. Israelachvili, H. Zeng, D. S. Hwang, *J. R. Soc., Interface* **2013**, *10*, 20120759.
- [42] a) R. J. Stewart, C. S. Wang, H. Shao, *Adv. Colloid Interface Sci.* **2011**, *167*, 85; b) R. A. Jensen, D. E. Morse, *J Comp Physiol B* **1988**, *158*, 317.
- [43] R. J. Stewart, J. C. Weaver, D. E. Morse, J. H. Waite, *J Exp Biol* **2004**, *207*, 4727.
- [44] J. H. Waite, R. A. Jensen, D. E. Morse, *Biochemistry* **1992**, *31*, 5733.
- [45] H. Zhao, C. Sun, R. J. Stewart, J. H. Waite, *J. Biol. Chem.* **2005**, *280*, 42938.
- [46] M. Gilbert, W. J. Shaw, J. R. Long, K. Nelson, G. P. Drobny, C. M. Giachelli, P. S. Stayton, *J. Biol. Chem.* **2000**, *275*, 16213.
- [47] M. Cui, S. Ren, S. Wei, C. Sun, C. Zhong, *APL Mater.* **2017**, *5*, 116102.
- [48] B. J. Endrizzi, R. J. Stewart, *J. Adhes.* **2009**, *85*, 546.
- [49] R. J. Stewart, C. S. Wang, I. T. Song, J. P. Jones, *Adv. Colloid Interface Sci.* **2017**, *239*, 88.
- [50] C. S. Wang, R. J. Stewart, *J Exp Biol* **2012**, *215*, 351.
- [51] a) H. J. Kim, B. Yang, T. Y. Park, S. Lim, H. J. Cha, *Soft Matter* **2017**, *13*, 7704; b) S. Chen, Q. Guo, J. Yu, *Aggregate* **2022**, *3*, 293.
- [52] B. Yang, S. Jin, Y. Park, Y. M. Jung, H. J. Cha, *Small* **2018**, *14*, 1803377.
- [53] Y. Jho, H. Y. Yoo, Y. Lin, S. Han, D. S. Hwang, *Adv. Colloid Interface Sci.* **2017**, *239*, 61.
- [54] N. Yonemura, F. Sehnal, K. Mita, T. Tamura, *Biomacromolecules* **2006**, *7*, 3370.
- [55] N. Yonemura, K. Mita, T. Tamura, F. Sehnal, *J. Mol. Evol.* **2009**, *68*, 641.
- [56] N. N. Ashton, H. Pan, R. J. Stewart, *Open Biol.* **2016**, *6*, 160067.
- [57] P. Flammang, A. Lambert, P. Bailly, E. Hennebert, *J. Adhes.* **2009**, *85*, 447.
- [58] P. B. Frandsen, M. G. Bursell, A. M. Taylor, S. B. Wilson, A. Steeneck, R. J. Stewart, *Philos. Trans. R. Soc., B* **2019**, *374*, 20190206.
- [59] J. B. Addison, N. N. Ashton, W. S. Weber, R. J. Stewart, G. P. Holland, J. L. Yarger, *Biomacromolecules* **2013**, *14*, 1140.

- [60] N. N. Ashton, D. R. Roe, R. B. Weiss, T. E. Cheatham III, R. J. Stewart, *Biomacromolecules* **2013**, *14*, 3668.
- [61] a) C.-S. Wang, N. N. Ashton, R. B. Weiss, R. J. Stewart, *Insect Biochem. Mol. Biol.* **2014**, *54*, 69; b) C.-S. Wang, H. Pan, G. M. Weerasekare, R. J. Stewart, *J. R. Soc., Interface* **2015**, *12*, 20150710.
- [62] D. Uzun, R. Ozyurt, Y. K. Demirel, O. Turan, *Appl. Ocean Res.* **2020**, *95*, 102020.
- [63] a) G. Walker, *J Mar Biol Assoc U K* **1972**, *52*, 429; b) K. Kamino, S. Odo, T. Maruyama, *Biol. Bull.* **1996**, *190*, 403.
- [64] M. J. Naldrett, *J Mar Biol Assoc U K* **1993**, *73*, 689.
- [65] J.-L. Jonker, J. von Byern, P. Flammang, W. Klepal, A. M. Power, *J Morphol* **2012**, *273*, 1377.
- [66] G. Walker, *Mar. Biol.* **1970**, *7*, 239.
- [67] C. R. So, J. M. Scancell, K. P. Fears, T. Essock-Burns, S. E. Haynes, D. H. Leary, Z. Diana, C. Wang, S. North, C. S. Oh, Z. Wang, B. Orihuela, D. Rittschof, C. M. Spillmann, K. J. Wahl, *ACS Appl. Mater. Interfaces* **2017**, *9*, 11493.
- [68] P. J. Cheung, G. D. Ruggieri, R. F. Nigrelli, *Mar. Biol.* **1977**, *43*, 157.
- [69] a) D. E. Barlow, G. H. Dickinson, B. Orihuela, J. L. Kulp, III, D. Rittschof, K. J. Wahl, *Langmuir* **2010**, *26*, 6549; b) R. M. A. Sullan, N. Gunari, A. E. Tanur, Y. Chan, G. H. Dickinson, B. Orihuela, D. Rittschof, G. C. Walker, *Biofouling* **2009**, *25*, 263.
- [70] M. Nakano, K. Kamino, *Biochemistry* **2015**, *54*, 826.
- [71] M. G. Iadanza, M. P. Jackson, E. W. Hewitt, N. A. Ranson, S. E. Radford, *Nat. Rev. Mol. Cell Biol.* **2018**, *19*, 755.
- [72] a) A. S. Mostaert, C. Giordani, R. Crockett, U. Karsten, R. Schumann, S. P. Jarvis, *J. Adhes.* **2009**, *85*, 465; b) M. M. Barnhart, M. R. Chapman, *Annu. Rev. Microbiol.* **2006**, *60*, 131.
- [73] C. R. So, J. Liu, K. P. Fears, D. H. Leary, J. P. Golden, K. J. Wahl, *ACS Nano* **2015**, *9*, 5782.
- [74] V. Sahni, T. A. Blackledge, A. Dhinojwala, *J. Adhes.* **2011**, *87*, 595.
- [75] M. Humenik, T. Scheibel, A. Smith, in *Prog. Mol. Biol. Transl. Sci.* (Ed: S. Howorka), Academic Press, New York **2011**, *103*, p. 131.
- [76] a) B. D. Opell, *J. Arachnol.* **1997**, *25*, 295; b) T. A. Blackledge, C. Y. Hayashi, *J Exp Biol* **2006**, *209*, 3131.
- [77] B. D. Opell, *Biol. J. Linn. Soc.* **1997**, *62*, 443.
- [78] T. A. Blackledge, N. Scharff, J. A. Coddington, T. Szüts, J. W. Wenzel, C. Y. Hayashi, I. Agnarsson, *Proc. Natl. Acad. Sci. USA* **2009**, *106*, 5229.
- [79] V. Sahni, T. A. Blackledge, A. Dhinojwala, *Nat. Commun.* **2010**, *1*, 19.
- [80] a) B. D. Opell, M. L. Hendricks, *J Exp Biol* **2010**, *213*, 339; b) F. Vollrath, W. J. Fairbrother, R. J. P. Williams, E. K. Tillinghast, D. T. Bernstein, K. S. Gallagher, M. A. Townley, *Nature* **1990**, *345*, 526; c) V. Sahni, T. Miyoshi, K. Chen, D. Jain, S. J. Blamires, T. A. Blackledge, A. Dhinojwala, *Biomacromolecules* **2014**, *15*, 1225.
- [81] G. Amarपुरi, V. Chaurasia, D. Jain, T. A. Blackledge, A. Dhinojwala, *Sci. Rep.* **2015**, *5*, 9030.
- [82] B. D. Opell, S. E. Karinshak, M. A. Sigler, *J Exp Biol* **2013**, *216*, 3023.
- [83] A. A. Walker, S. Weisman, H. E. Trueman, D. J. Merritt, T. D. Sutherland, *Comp. Biochem. Physiol., Part B: Biochem. Mol. Biol.* **2015**, *187*, 78.
- [84] J. A.-O. von Byern, V. Dorner, D. J. Merritt, P. Chandler, I. Stringer, M. Marchetti-Deschmann, A. McNaughton, N. Cyran, K. Thiel, M. Noeske, I. Grunwald, *PLoS One* **2016**, *11*.
- [85] S. W. Taylor, J. H. Waite, M. M. Ross, J. Shabanowitz, D. F. Hunt, *J. Am. Chem. Soc.* **1994**, *116*, 10803.
- [86] K. Inoue, Y. Takeuchi, D. Miki, S. Odo, *J. Biol. Chem.* **1995**, *270*, 6698.
- [87] V. V. Papov, T. V. Diamond, K. Biemann, J. H. Waite, *J. Biol. Chem.* **1995**, *270*, 20183.
- [88] H. Zhao, J. H. Waite, *Biochemistry* **2006**, *45*, 14223.
- [89] H. Zhao, J. H. Waite, *J. Biol. Chem.* **2006**, *281*, 26150.
- [90] N. N. Ashton, D. S. Taggart, R. J. Stewart, *Biopolymers* **2011**, *97*, 432.
- [91] a) H. Mohanram, A. Kumar, C. S. Verma, K. Pervushin, A. Miserez, *Philos. Trans. R. Soc., B* **2019**, *374*, 20190198; b) K. Kamino, *Biochem. J.* **2001**, *356*, 503.
- [92] Y. Mu, Q. Sun, B. Li, X. Wan, *Polym. Rev.* **2023**, *63*, 1.
- [93] J. J. Castillo, B. K. Shanbhag, L. He, in *Food Bioactives: Extraction and Biotechnology Applications* (Ed: M. Puri), Springer International Publishing, Cham **2017**, p. 111.
- [94] H. Lee, S. M. Dellatore, W. M. Miller, P. B. Messersmith, *Science* **2007**, *318*, 426.
- [95] a) E. M. Alberts, P. U. A. I. Fernando, T. L. Thornell, H. E. George, A. M. Koval, M. K. Shukla, C. A. Weiss, L. C. Moores, *R Soc Open Sci* **2022**, *9*, 211637; b) L. J. Duan, Y. Liu, J. Kim, D. J. Chung, *J. Appl. Polym. Sci.* **2013**, *130*, 131.
- [96] S. Bai, X. Zhang, P. Cai, X. Huang, Y. Huang, R. Liu, M. Zhang, J. Song, X. Chen, H. Yang, *Nanoscale Horiz.* **2019**, *4*, 1333.
- [97] J. Sun, L. Xiao, B. Li, K. Zhao, Z. Wang, Y. Zhou, C. Ma, J. Li, H. Zhang, A. Herrmann, K. Liu, *Angew. Chem., Int. Ed.* **2021**, *60*, 23687.
- [98] L. Ninan, J. Monahan, R. L. Strohshine, J. J. Wilker, R. Shi, *Biomaterials* **2003**, *24*, 4091.
- [99] C. Sun, G. E. Fantner, J. Adams, P. K. Hansma, J. H. Waite, *J Exp Biol* **2007**, *210*.
- [100] B. Zhao, Q. Chen, G. Da, J. Yao, Z. Shao, X. Chen, *J. Mater. Chem. C* **2021**, *9*, 8955.
- [101] H. Liu, M. Yuan, J. Sonamuthu, S. Yan, W. Huang, Y. Cai, J. Yao, *New J. Chem.* **2020**, *44*, 884.
- [102] Z. Yin, H. Liu, M. Lin, W. Xie, X. Yang, Y. Cai, *Biomed. Mater.* **2021**, *16*, 045025.
- [103] Z. Bashir, W. Yu, Z. Xu, Y. Li, J. Lai, Y. Li, Y. Cao, B. Xue, *Int. J. Mol. Sci.* **2022**, *23*, 9987.
- [104] Y. S. Choi, Y. J. Yang, B. Yang, H. J. Cha, *Microb. Cell Fact.* **2012**, *11*, 139.
- [105] W. H. Park, J. Lee, H. J. Kim, K. I. Joo, H. J. Cha, *Chem. Eng. J.* **2022**, *446*, 137272.
- [106] C. Liang, Z. Ye, B. Xue, L. Zeng, W. Wu, C. Zhong, Y. Cao, B. Hu, P. B. Messersmith, *ACS Appl. Mater. Interfaces* **2018**, *10*, 25017.
- [107] V. G. Bogush, L. I. Davydova, V. S. Shulyakov, K. V. Sidoruk, S. V. Krashenninnikov, M. A. Bychkova, V. G. Debabov, *Appl. Biochem. Microbiol.* **2022**, *58*, 842.
- [108] P. Aich, J. An, B. Yang, Y. H. Ko, J. Kim, J. Murray, H. J. Cha, J. H. Roh, K. M. Park, K. Kim, *Chem. Commun.* **2018**, *54*, 12642.
- [109] E. Kim, J. Jeon, Y. Zhu, E. D. Hoppe, Y.-S. Jun, G. M. Genin, F. Zhang, *ACS Appl. Mater. Interfaces* **2021**, *13*, 48457.
- [110] P. Mohammadi, G. Beaune, B. T. Stokke, J. V. I. Timonen, M. B. Linder, *ACS Macro Lett.* **2018**, *7*, 1120.
- [111] C. Ma, J. Sun, B. Li, Y. Feng, Y. Sun, L. Xiang, B. Wu, L. Xiao, B. Liu, V. S. Petrovskii, L. Bin, J. Zhang, Z. Wang, H. Li, L. Zhang, J. Li, F. Wang, R. Göstl, I. I. Potemkin, D. Chen, H. Zeng, H. Zhang, K. Liu, A. Herrmann, *Nat. Commun.* **2021**, *12*.
- [112] Z. Wang, X. Gu, B. Li, J. Li, F. Wang, J. Sun, H. Zhang, K. Liu, W. Guo, *Adv. Mater.* **2022**, *34*, 2204590.
- [113] K. Zhao, Y. Liu, Y. Ren, B. Li, J. Li, F. Wang, C. Ma, F. Ye, J. Sun, H. Zhang, K. Liu, *Angew. Chem., Int. Ed.* **2022**, *134*, 202207425.
- [114] Z. Wei, J. Sun, S. Lu, Y. Liu, B. Wang, L. Zhao, Z. Wang, K. Liu, J. Li, J. Su, F. Wang, H. Zhang, Y. Yang, *Adv. Mater.* **2022**, *34*, 2110062.
- [115] S. H. Kim, Y. J. Lee, J. R. Chao, D. Y. Kim, M. T. Sultan, H. J. Lee, J. M. Lee, J. S. Lee, O. J. Lee, H. Hong, H. Lee, O. Ajiteru, Y. J. Suh, H. S. Choi, Y.-J. Cho, C. H. Park, *NPG Asia Mater.* **2020**, *12*, 46.
- [116] D. S. Hwang, Y. Gim, H. J. Yoo, H. J. Cha, *Biomaterials* **2007**, *28*, 3560.
- [117] B.-H. Choi, H. Cheong, Y. K. Jo, S. Y. Bahn, J. H. Seo, H. J. Cha, *Microb. Cell Fact.* **2014**, *13*, 52.
- [118] B. Yang, N. Ayyadurai, H. Yun, Y. S. Choi, B. H. Hwang, J. Huang, Q. Lu, H. Zeng, H. J. Cha, *Angew. Chem., Int. Ed.* **2014**, *53*, 13360.

- [119] a) Y. K. Jo, B.-H. Choi, C. Zhou, J.-S. Ahn, S. H. Jun, H. J. Cha, *J. Mater. Chem. B* **2015**, 3, 8102; b) D. Hwang, S. B. Sim, H. J. Cha, *Biomaterials* **2007**, 28, 4039.
- [120] J. Wang, T. Scheibel, *Biotechnol. J.* **2018**, 13, 1800146.
- [121] S. C. T. Nicklisch, S. Das, N. R. Martinez Rodriguez, J. H. Waite, J. N. Israelachvili, *Biotechnol. Prog.* **2013**, 29, 1587.
- [122] X. Li, J. Mi, R. Wen, J. Zhang, Y. Cai, Q. Meng, Y. Lin, *ACS Appl Bio Mater* **2020**, 3, 5957.
- [123] T. I. Harris, D. A. Gaztambide, B. A. Day, C. L. Brock, A. L. Ruben, J. A. Jones, R. V. Lewis, *Biomacromolecules* **2016**, 17, 3761.
- [124] a) C. J. Love, B. A. Serban, T. Katashima, K. Numata, M. A. Serban, *ACS Biomater. Sci. Eng.* **2019**, 5, 5960; b) A. D. Roberts, W. Finnigan, P. P. Kelly, M. Faulkner, R. Breitling, E. Takano, N. S. Scrutton, J. J. Blaker, S. Hay, *Mater Today Bio* **2020**, 7, 100068.
- [125] Y. Liu, A. Sponner, D. Porter, F. Vollrath, *Biomacromolecules* **2008**, 9, 116.
- [126] D. Porro, B. Gasser, T. Fossati, M. Maurer, P. Branduardi, M. Sauer, D. Mattanovich, *Appl. Microbiol. Biotechnol.* **2011**, 89, 939.
- [127] a) X. Zheng, W. W. Fan, L. J. Meng, S. S. Li, Y. Y. Liu, L. H. Zhang, *Adv. Mater. Res.* **2012**, 581–582, 1137; b) N. Bolghari, H. Shamsavarani, M. Anvari, H. Habibollahi, *AMB Express* **2022**, 12, 1.
- [128] N. Lang, M. J. Pereira, Y. Lee, I. Friehs, N. V. Vasilyev, E. N. Feins, K. Ablasser, E. D. O’Cearbhaill, C. Xu, A. Fabozzo, R. Padera, S. Wasserman, F. Freudenthal, L. S. Ferreira, R. Langer, J. M. Karp, P. J. del Nido, *Sci. Transl. Med.* **2014**, 6, 218.
- [129] E. Y. Jeon, B. H. Hwang, Y. J. Yang, B. J. Kim, B.-H. Choi, G. Y. Jung, H. J. Cha, *Biomaterials* **2015**, 67, 11.
- [130] H. Cheong, Y.-J. Jun, E. Y. Jeon, J. I. Lee, H. J. Jo, H. Y. Park, E. Kim, J. W. Rhie, K. I. Joo, H. J. Cha, *Chem. Eng. J.* **2022**, 445, 136641.
- [131] S.-W. Maeng, T. Y. Park, J. S. Min, L. Jin, K. I. Joo, W. C. Park, H. J. Cha, *Adv. Healthcare Mater.* **2021**, 10, 2100100.
- [132] M. Hauf, F. Richter, T. Schneider, T. Faidt, B. M. Martins, T. Baumann, P. Durkin, H. Dobbek, K. Jacobs, A. Möglich, N. Budisa, *ChemBioChem* **2017**, 18, 1819.
- [133] Y. Guo, Y. Wang, X. Zhao, X. Li, Q. Wang, W. Zhong, K. Mequanint, R. Zhan, M. Xing, G. Luo, *Sci. Adv.* **2021**, 7, eabf9635.
- [134] M. J. Brennan, B. F. Kilbride, J. J. Wilker, J. C. Liu, *Biomaterials* **2017**, 124, 116.
- [135] L. Xiao, Z. Wang, Y. Sun, B. Li, B. Wu, C. Ma, V. S. Petrovskii, X. Gu, D. Chen, I. I. Potemkin, A. Herrmann, H. Zhang, K. Liu, *Angew. Chem., Int. Ed.* **2021**, 133, 12189.
- [136] E. Y. Jeon, K. I. Joo, H. J. Cha, *Acta Biomater.* **2020**, 114, 244.
- [137] L. Zhou, C. Dai, L. Fan, Y. Jiang, C. Liu, Z. Zhou, P. Guan, Y. Tian, J. Xing, X. Li, Y. Luo, P. Yu, C. Ning, G. Tan, *Adv. Funct. Mater.* **2021**, 31, 2007457.
- [138] S. Arias, S. Amini, J. Horsch, M. Pretzler, A. Rompel, I. Melnyk, D. Sychev, A. Fery, H. G. Börner, *Angew. Chem., Int. Ed.* **2020**, 59, 18495.
- [139] A. R. Narkar, B. Barker, M. Clisch, J. Jiang, B. P. Lee, *Chem. Mater.* **2016**, 28, 5432.
- [140] X. Xu, X. Xia, K. Zhang, A. Rai, Z. Li, P. Zhao, K. Wei, L. Zou, B. Yang, W.-K. Wong, P. W.-Y. Chiu, L. Bian, *Sci. Transl. Med.* **2020**, 12, eaba8014.
- [141] H. Yuk, C. E. Varela, C. S. Nabzdyk, X. Mao, R. F. Padera, E. T. Roche, X. Zhao, *Nature* **2019**, 575, 169.
- [142] H. Q. Pham, M. J. Marks, in *Ullmann’s Encyclopedia of Industrial Chemistry*, Wiley, Hoboken **2005**.
- [143] L. Kortekaas, J. Simke, D. W. Kurka, B. J. Ravoo, *ACS Appl. Mater. Interfaces* **2020**, 12, 32054.
- [144] Q. Zhu, X. Zhou, Y. Zhang, D. Ye, K. Yu, W. Cao, L. Zhang, H. Zheng, Z. Sun, C. Guo, X. Hong, Y. Zhu, Y. Zhang, Y. Xiao, T. G. Valencak, T. Ren, D. Ren, *Biomater. Res.* **2023**, 27, 6.
- [145] J. Liu, H. Sheha, Y. Fu, L. Liang, S. C. G. Tseng, *Expert Rev. Ophthalmol.* **2010**, 5, 645.
- [146] B. Li, D. O. V. Alonso, V. Daggett, *J. Mol. Biol.* **2001**, 305, 581.
- [147] a) T. Duan, H. Li, *Biomacromolecules* **2020**, 21, 2258; b) L. Chambre, Z. Martín-Moldes, R. N. Parker, D. L. Kaplan, *Adv. Drug Delivery Rev.* **2020**, 160, 186.
- [148] B. Trzebicka, R. Szweda, D. Kosowski, D. Szweda, Ł. Otulakowski, E. Haladjova, A. Dworak, *Prog. Polym. Sci.* **2017**, 68, 35.
- [149] J. He, Z. Zhang, Y. Yang, F. Ren, J. Li, S. Zhu, F. Ma, R. Wu, Y. Lv, G. He, B. Guo, D. Chu, *Nano-Micro Lett.* **2021**, 13, 80.
- [150] M. Krogsgaard, M. A. Behrens, J. S. Pedersen, H. Birkedal, *Biomacromolecules* **2013**, 14, 297.
- [151] R. Wang, B. Jiang, F. Sun, *Matter* **2020**, 3, 1820.
- [152] B. An, Y. Wang, X. Jiang, C. Ma, M. Mimee, F. Moser, K. Li, X. Wang, T.-C. Tang, Y. Huang, Y. Liu, T. K. Lu, C. Zhong, *Matter* **2020**, 3, 2080.
- [153] C. Zhang, J. Huang, J. Zhang, S. Liu, M. Cui, B. An, X. Wang, J. Pu, T. Zhao, C. Fan, T. K. Lu, C. Zhong, *Mater. Today* **2019**, 28, 40.



**Christina Heinritz** received both her B.Sc. degree in biochemistry (2018) and her M.Sc. in biochemistry and molecular biology (2021) from the University of Bayreuth (Germany). She is currently a Ph.D. candidate at University of Bayreuth (Germany) under the supervision of Thomas Scheibel and her current research focuses on spider silk-based recombinant proteins and their use in the development of engineered tissues with vascular supply.



**Xuen J. Ng** received his B.Sc. degree in biology (2017) and his M.Sc. in biochemistry and molecular biology (2020) in cooperation with CSIRO (Clayton Melbourne, Australia) at the University of Bayreuth. He is currently a Ph.D. candidate at the Department of Biomaterials under the supervision of Prof. Dr. Thomas Scheibel and investigates the use and development of recombinant spider silk-based bioinks for application in cardiac tissue engineering.



**Thomas Scheibel** is a full professor for Biomaterials as well as Vice President for research and junior scholars at the University of Bayreuth. Since 2014 he is a member of the German National Academy of Science and Engineering (Acatech). He initiated and chairs the topical committee on “Bioinspired and interactive materials” at the German Materials Society (DGM), is chairman of the Bavarian Excellence Network “Cellular Hybrids”, co-chairman of the TranregioSFB TRR225 “Biofabrication”, and Member of the review board “biomaterials” of the DFG.